The Plant Cell, Vol. 22: 606–622, March 2010, www.plantcell.org © 2010 American Society of Plant Biologists

F-Box Proteins FKF1 and LKP2 Act in Concert with ZEITLUPE to Control *Arabidopsis* Clock Progression [C][W]

Antoine Baudry,[a] Shogo Ito,[b] Young Hun Song,[b] Alexander A. Strait,[b] Takatoshi Kiba,[c,1] Sheen Lu,[d] Rossana Henriques,[c] José L. Pruneda-Paz,[a] Nam-Hai Chua,[c] Elaine M. Tobin,[d] Steve A. Kay,[a] and Takato Imaizumi[b,2]

[a] Section of Cell and Developmental Biology, Division of Biological Sciences, University of California at San Diego, La Jolla, California 92093

[b] Department of Biology, University of Washington, Seattle, Washington 98195

[c] Laboratory of Plant Molecular Biology, Rockefeller University, New York, New York 10065

[d] Department of Molecular, Cell, and Developmental Biology, University of California, Los Angeles, California 90095

Regulation of protein turnover mediated by ZEITLUPE (ZTL) constitutes an important mechanism of the circadian clock in *Arabidopsis thaliana*. Here, we report that FLAVIN BINDING, KELCH REPEAT, F-BOX1 (FKF1) and LOV KELCH PROTEIN2 (LKP2) play similar roles to ZTL in the circadian clock when ZTL is absent. In contrast with subtle circadian clock defects in *fkf1*, the clock in *ztl fkf1* has a considerably longer period than in *ztl*. In *ztl fkf1 lkp2*, several clock parameters were even more severely affected than in *ztl fkf1*. Although *LATE ELONGATED HYPOCOTYL* (*LHY*) and *CIRCADIAN CLOCK ASSOCIATED1* (*CCA1*) expression levels are lower in *ztl* than in the wild type, introducing both *fkf1* and *lkp2* mutations into the *ztl* mutant dramatically diminished *LHY* expression without further affecting *CCA1* expression. This demonstrates different contributions of ZTL, FKF1, and LKP2 in the regulation of *LHY* and *CCA1* expression. In addition, FKF1 and LKP2 also interacted with TIMING OF CAB EXPRESSION1 (TOC1) and PSEUDO-RESPONSE REGULATOR5 (PRR5), and both proteins were further stabilized in *ztl fkf1* and *ztl fkf1 lkp2* compared with in *ztl*. Our results indicate that ZTL, FKF1, and LKP2 together regulate TOC1 and PRR5 degradation and are major contributors to determining the period of circadian oscillation and enhancing robustness.

INTRODUCTION

Endogenous time keepers known as circadian clocks underlie daily and seasonal changes in the physiology and behaviors of terrestrial organisms from cyanobacteria to humans (Bell-Pedersen et al., 2005; Wijnen and Young, 2006). Plant circadian biology has been instrumental in demonstrating the numerous advantages conferred by these internal oscillators, as well as their impact on an organism's fitness (Green et al., 2002; Michael et al., 2003; Dodd et al., 2005; Ni et al., 2009). This contribution to growth vigor can be explained by clock action on a variety of outputs, such as gene expression, calcium ion fluxes, metabolic activities (including photosynthesis), hormone production and signaling, stress responses, organ movements, and transition to flowering (Baudry and Kay, 2008; Harmer, 2009; Imaizumi, 2010). Extensive microarray experiments showed that the key action of the clock is to establish numerous gene expression programs oscillating with an ~24-h period (Baudry and Kay, 2008; Más, 2008; Harmer, 2009). Affecting the expression of nearly one-third of protein coding sequences in *Arabidopsis thaliana*, the clock plays an important role in coordinating plant gene expression with light, temperature, and nutrient availability (Bläsing et al., 2005; Michael et al., 2008).

At its core, the plant circadian oscillator is composed of several partially redundant feedback loops, which form a complex gene network of transcription factors and proteins closely associated with the transcription machinery (Más, 2008; Harmer, 2009). The morning expressed MYB transcription factors, *CIRCADIAN CLOCK ASSOCIATED1* (*CCA1*) and *LATE ELONGATED HYPOCOTYL* (*LHY*) compose a negative arm of the first characterized loop (Alabadi et al., 2001). Directly repressing the transcription of *TIMING OF CAB EXPRESSION1* (*TOC1*; Makino et al., 2000; Strayer et al., 2000) and several other evening genes, CCA1/LHY specifically bind to a *cis*-element called the evening element (Alabadi et al., 2001) and affect histone acetylation (Perales and Más, 2007). *TOC1*, also known as *PSEUDO-RESPONSE REGULATOR1* (*PRR1*; Makino et al., 2000), in turn participates in *CCA1* and *LHY* activation at dawn (Alabadi et al., 2001) potentially by directly modulating transcription factor activity (Pruneda-Paz et al., 2009). At least two additional loops feed back to *CCA1/LHY* by repressing their expression, thus allowing the progression of the oscillator. One is composed of *PRR7* and *PRR9* (Farré et al., 2005; Salomé and McClung, 2005), two partially redundant members of the *PRR* family that are

[1] Current address: RIKEN Plant Science Center, Tsurumi, Yokohama 230-0045, Japan.

[2] Address correspondence to takato@u.washington.edu.

The authors responsible for distribution of materials integral to the findings presented in this article in accordance with the policy described in the Instructions for Authors (www.plantcell.org) are: Steve A. Kay (skay@ucsd.edu) and Takato Imaizumi (takato@u.washington.edu).

[C]Some figures in this article are displayed in color online but in black and white in the print edition.

[W]Online version contains Web-only data.

www.plantcell.org/cgi/doi/10.1105/tpc.109.072843

transcriptionally activated by CCA1 and LHY in the morning. The second loop integrates a recently characterized transcription factor named *CHE* (for *CCA1 HIKING EXPEDITION*) that belongs to the TCP family (for TB1, CYC, PCF; Pruneda-Paz et al., 2009). CHE forms a protein complex with TOC1 that specifically regulates *CCA1* transcription. In addition, several other clock components have been identified that contribute to *CCA1/LHY* oscillations (Baudry and Kay, 2008). The list includes EARLY FLOWERING3 (ELF3), ELF4 proteins, and the LUX ARRHYTHMO (LUX) MYB-domain transcription factor, although these factors still need to be clearly positioned within the circadian network (Covington et al., 2001; Doyle et al., 2002; Hazen et al., 2005).

Fine-tuning of protein turnover is an additional hallmark of the molecular mechanisms at the core of the oscillator (Más, 2008; Harmer, 2009). Genetic screens have identified ZEITLUPE (ZTL; Somers et al., 2000), an F-box protein that possesses a light-regulated protein interaction domain called the LOV (Light, Oxygen, or Voltage) domain at its N terminus (Imaizumi et al., 2003; Kim et al., 2007). This domain is responsible for specifically anchoring TOC1 and PRR5, another member of the PRR family, and targeting both proteins for proteasome-dependent degradation (Más et al., 2003b; Kiba et al., 2007). However, during the day, blue light induces the LOV domain of ZTL to favor interacting with GIGANTEA (GI), thus protecting TOC1, PRR5, and ZTL from degradation until dusk (Kim et al., 2007). Thereafter, a delaying mechanism involving PRR3 specifically affects TOC1 by slowing down its degradation until the middle of the night (Para et al., 2007; Fujiwara et al., 2008). PRR3 prevents ZTL-TOC1 interaction by directly binding to the ZTL-interacting domain of TOC1. These light-modulated posttranslational mechanisms participate in refining TOC1 and PRR5 protein oscillations. ZTL is thus an indirect but important factor in the determination of the period of the oscillator, as well as of the transcription of several core clock genes.

A remarkably similar sequence of interactions takes place between GI and FLAVIN BINDING, KELCH REPEAT, F-BOX1 (FKF1; Nelson et al., 2000) in the regulation of photoperiodic flowering. Homologous to ZTL, FKF1 also interacts with GI through the LOV domain in a blue light–dependent manner (Sawa et al., 2007). The formation of the GI-FKF1 complex becomes optimal in long-day afternoons after synchronization of the clock-controlled transcription of these two genes. Simultaneous interaction through the kelch repeats (another signature domain at the C-terminal end of FKF1) and with the N-terminal portion of GI allows the recruitment and degradation of CYCLING DOF FACTOR1 (CDF1; Imaizumi et al., 2005; Sawa et al., 2007), as well as several other Dof (DNA binding with one zinc-finger) factors homologous to CDF1 (Fornara et al., 2009). Directly repressing the expression of the floral integrator *CONSTANS* (*CO*), CDF1 binds to specific regions of the *CO* promoter (Imaizumi et al., 2005), where the GI-FKF1-CDF1 complex is thought to be assembled (Sawa et al., 2007). Alleviating *CO* repression during the daytime, FKF1 and GI participate in the early steps of flowering induction by extended photoperiods and are key components in the mechanisms leading to daylength discrimination.

A third member of the ZTL family of F-box proteins named LOV KELCH PROTEIN2 (LKP2) is present in *Arabidopsis* (Schultz et al., 2001; Imaizumi et al., 2003; Yasuhara et al., 2004). Interestingly, LKP2 homologs are also found in rice (*Oryza sativa*) and poplar (*Populus trichocarpa*; Xu et al., 2009), suggesting that all members of the ZTL clade are conserved among plants. Similarly to ZTL and FKF1, LKP2 interacts with GI through its LOV domain (Kim et al., 2007) and has relatively conserved kelch repeats. Despite clock-associated properties similar to ZTL revealed after overexpression in planta (Schultz et al., 2001), the real function of LKP2 remains uncertain because no clock defect has been described in the *lkp2* mutant. Consistent with its clock action, LKP2 interacts in vitro with TOC1 and PRR5 (Más et al., 2003b; Yasuhara et al., 2004), but it also shares functional features with FKF1 by interacting with several CDFs (Imaizumi et al., 2005) and being detected in the nucleus (Fukamatsu et al., 2005). Several studies have highlighted complex functional redundancies among homologous F-box proteins (Dharmasiri et al., 2005; Schwager et al., 2007; Qiao et al., 2009). Indeed, a recent study reported a moderate enhancement of the *fkf1* late-flowering phenotype in plants also mutated for *ZTL* and *LKP2* (Fornara et al., 2009), indicating that some functionalities are shared by all the members of this small gene family.

In this study, we addressed the potential redundancy between ZTL, FKF1, and LKP2 in the *Arabidopsis* clockwork. All mutant combinations were obtained by crosses and carefully compared for the activity of several clock outputs. *LKP2* function was investigated by looking at *lkp2* and *ztl lkp2* phenotypes, but we were unable to reveal any clock differences in these backgrounds when compared with the appropriate controls. By contrast, a strong enhancement of the *ztl* long-period phenotype was detected in the *ztl fkf1* double mutant, with a 2-h extension of the oscillator period. This result was unexpected because, unlike *LKP2*, *FKF1* was unable to complement the *ztl* mutant when increased levels of expression were conferred by the *ZTL* promoter. Still, protein immunoblotting using anti-TOC1 and anti-PRR5 antibodies indicated increased levels of these two proteins in *ztl fkf1*, thus demonstrating that FKF1 acts on the clock through the same targets as ZTL. In addition, several clock parameters were more severely affected in the *ztl fkf1 lkp2* triple mutant than in *ztl fkf1*, resulting in weak rhythms for several outputs. Together, our results suggest a complex redundancy mechanism between *ZTL*, *FKF1*, and *LKP2*, probably due in part to the large differences in the expression levels of these genes. Finally, the remarkably enhanced phenotype characterized in the triple mutant gave us the opportunity to analyze precisely their functions within the *Arabidopsis* circadian network. We provide a comprehensive analysis of the triple mutant phenotype, assigning contrasting functions to the main targets of this conserved family of F-box proteins, TOC1 and PRR5.

RESULTS

Despite a Functional Homology with ZTL, LKP2 Seems Dispensable to the Clock

To assess LKP2 function in the *Arabidopsis* clockwork, we first characterized *lkp2*, a T-DNA insertion mutant completely devoid of *LKP2* expression (Imaizumi et al., 2005). The circadian reporter *CAB2:LUC* (for *CHLOROPHYLL A/B BINDING PROTEIN2* promoter fused to the luciferase gene) was introduced by crossing,

and its activity was monitored in this mutant background. After 5 d in constant light (LL) conditions, *CAB2:LUC* oscillations in *lkp2* presented no difference when compared with the oscillations in wild-type plants (Figure 1A). Similarly, the rhythm of *CCA1* transcription was not affected (Figure 1C), suggesting that the core oscillator and clock outputs are unchanged in these plants. Microarray experiments (eFP browser; http://bbc.cagef.utoronto.ca/) and promoter activities (Kiyosue and Wada, 2000; Schultz et al., 2001; Yasuhara et al., 2004) indicate that *ZTL* and *LKP2* expression domains are overlapping and suggest that a role for LKP2 in a tissue-specific clock function is unlikely. However, by monitoring variations in the mRNA copy number of these genes during the first 24 h in LL, we found considerable differences in their expression levels in wild-type plants (Figure 2A). With a stable expression of 6663 copies/ng of total RNA on average, *ZTL* was the most highly expressed. By contrast, average *LKP2* expression corresponded to only 4% of *ZTL* levels with 262 copies/ng of total RNA. In addition, we analyzed whether this large difference in mRNA copy number between the *ZTL* and *LKP2* transcripts exists in the mutant backgrounds. *ZTL* expression level was largely unaffected by the *lkp2* mutation (see Supplemental Figure 1A online). Similarly, *LKP2* expression level in the *ztl* mutant resembled that in the wild-type plants (see Supplemental Figure 1B online).

To test if the low levels of *LKP2* transcripts could be responsible for reduced activity in plants, *LKP2* cDNA was placed under the control of the *ZTL* promoter and introduced into the *ztl* mutant. This construct successfully complemented the long period phenotype of *ztl* (Figure 2B), indicating that ZTL and LKP2 are functionally homologous proteins. Interestingly, a wide distribution of period lengths was observed in the T1 seedlings in which either *LKP2* or *ZTL* was expressed (Figure 2B). Based on the previously characterized ZTL dosage-dependent regulation of circadian period length (Somers et al., 2004), our data suggested that we obtained an allelic series with a gradation in the levels of expression of *ZTL* and *LKP2*. *ZTL* seemed more efficient than *LKP2* in reverting the *ztl* long-period phenotype, even generating a consequent subset of seedlings with a very short period (12 out of 35 T1 plants with an estimated period length lower than 20 h; Figure 2B). In addition, measuring *LKP2* mRNA copy number in the *ZTL:LKP2/ztl* lines with periods close to the wild type, we found that these lines possessed ~1.5 times more *LKP2* transcript than the sum of both *ZTL* and *LKP2* mRNA copy numbers in the wild type (Figure 2C). This indicates that

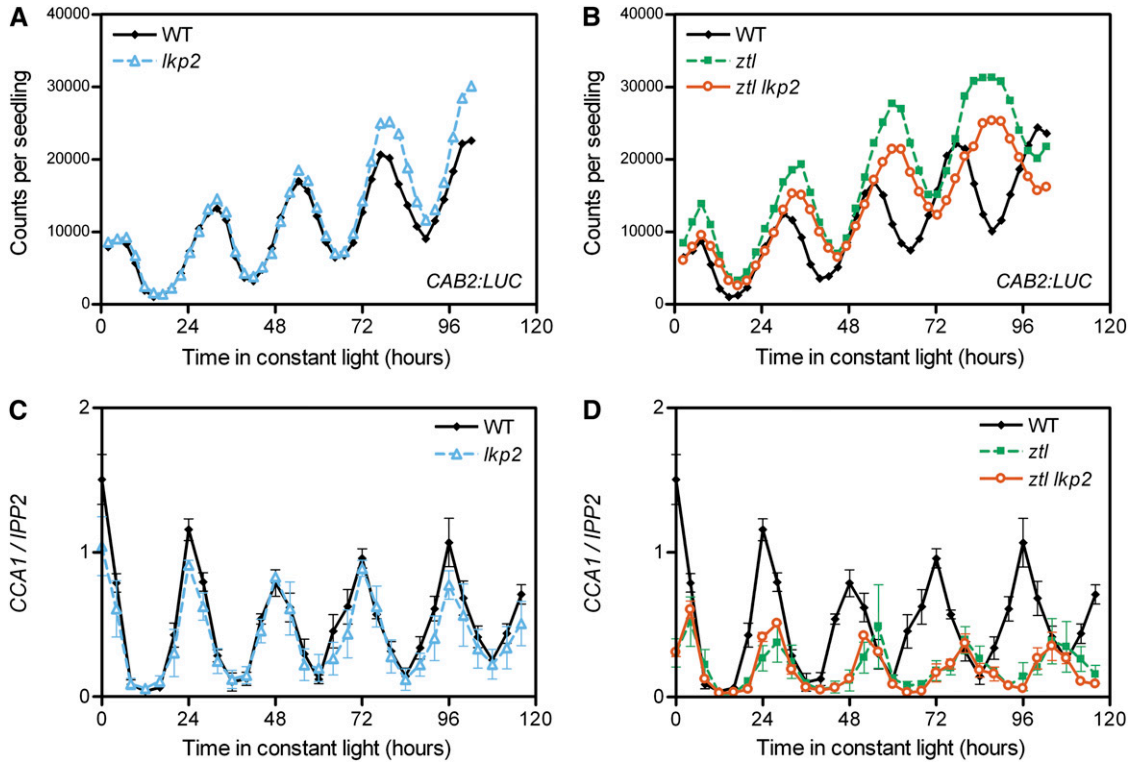

Figure 1. Analysis of *lkp2* and *ztl lkp2* Clock Phenotypes.

CAB2:LUC activity (**[A]** and **[B]**) and *CCA1* expression (**[C]** and **[D]**) were analyzed in wild-type, *lkp2*, *ztl*, and *ztl lkp2* plants in constant light (LL) conditions.

(A) and **(B)** *CAB2:LUC* traces represent the average of the results obtained for 36 seedlings of each genotype and are representative of three independent experiments.

(C) and **(D)** Normalized *CCA1* expression level is the average (±SE) of three independent biological replicates measured by real-time RT-PCR.

[See online article for color version of this figure.]

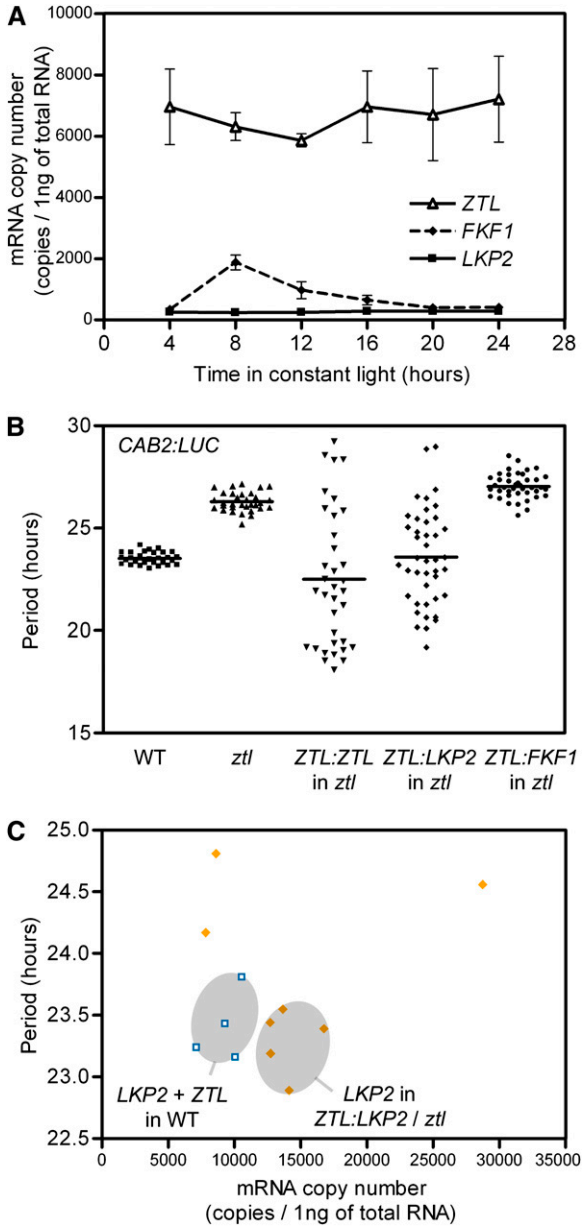

Figure 2. *ztl* Complementation Experiment.

(A) *ZTL*, *FKF1*, and *LKP2* mRNA copy numbers in the wild type are the average (± SDEV) of three biological replicates and were determined for the first 24 h in LL conditions.

(B) Scatterplot of the period of *CAB2:LUC* oscillations in LL in the wild type (n = 32), *ztl* (n = 32), and T1 *ztl* plants harboring either *ZTL:ZTL* (n = 35), *ZTL:LKP2* (n = 42), or *ZTL:FKF1* (n = 41) constructs.

(C) Sum of *ZTL* and *LKP2* mRNA copy numbers in leaves of wild-type plants (open symbols, n = 4) is compared with the levels of *LKP2* in *ZTL:LKP2* T1 plants (closed symbols, n = 8), which showed a similar period length to the average period of wild-type plants. The gray circles depict the distribution of wild-type data and the *ZTL:LKP2* individuals that have a similar period length to wild-type plants.

[See online article for color version of this figure.]

more mRNA copies of *LKP2* are required to replace endogenous ZTL function. In other words, the role of ZTL in the clock could be substituted by LKP2, but the functions of ZTL and LKP2 are not fully equivalent.

A potential redundancy between *ZTL* and *LKP2* was further addressed by the characterization of the *ztl lkp2* double mutant. These plants were indistinguishable from the *ztl* mutant and presented the same 3-h period lengthening for *CAB2:LUC* reporter or *CCA1* expression (Figures 1B and 1D). They also displayed a reduction in *CCA1* expression to 50% of wild-type peak levels, similar to the *ztl* mutants. Considering the functional similarity between ZTL and LKP2 and also the large difference in the mRNA copy number between their respective transcripts, these results indicate that the loss of *LKP2* might cause too small of an impact on the clock progression to be detected. Another possibility is that an additional factor prevents the *lkp2* mutation from having any noticeable defect in the *ztl lkp2* plants.

fkf1 Mutation Enhances the *ztl* Clock Phenotype

In contrast with the *ztl lkp2* mutant, a more severe clock phenotype was observed in the *ztl fkf1* double mutant. First, the period of *CAB2:LUC* oscillation displayed a 2-h lengthening when compared with *ztl* and a 5-h delay compared with wild-type plants (Figures 3B and 4B). Another clock output, leaf movement rhythms, also displayed a much longer period phenotype in *ztl fkf1* than in *ztl* (Figure 4C). When we analyzed the expression of several core clock genes, consistent similar alterations in period length were observed, as well as unexpectedly low expression levels for some of the morning genes. *LHY* and *PRR9* were the more dramatically affected, with peak levels of expression corresponding to 10% of the wild-type levels in *ztl fkf1* (Figures 3E and 3F). *PRR7* and *CCA1* were also reduced to 30 and 50% of their respective wild-type peak levels (Figure 3D; see Supplemental Figure 2B online). Although similar low levels were seen in *ztl* for *PRR9*, *PRR7*, and *CCA1*, the reduction of *LHY* was more severe in *ztl fkf1* (from 20 to <10%), suggesting that this *LHY* difference may contribute to the additive clock phenotype in the *ztl fkf1* mutant.

The *fkf1*-dependent clock defect, which is pronounced only with the presence of the *ztl* mutation, prompted us to investigate further the single mutant phenotype. After 4 d in LL, a minor lagging of the peak of *CAB2:LUC* was seen in *fkf1* (Figure 3A), indicating a subtle period change. As an increase in the lengthening of the period has been shown with decreasing fluences of light for *ztl* (Somers et al., 2000, 2004), we tested whether lowering the fluences of white light enable an enhancement of the *fkf1* clock phenotype. In our experiment, the 3-h period lengthening seen for *ztl* in regular conditions (90 $\mu mol \cdot m^{-2} \cdot s^{-1}$) increased to 3 h 30 min at the lower fluence (4 $\mu mol \cdot m^{-2} \cdot s^{-1}$) but was closer to 2 h at the highest fluence (176 $\mu mol \cdot m^{-2} \cdot s^{-1}$; Figure 3C). For *fkf1*, a 20-min period difference on average was observed at 90 $\mu mol \cdot m^{-2} \cdot s^{-1}$, and this difference gradually increased and became more noticeable (up to a 1 h difference) with lower fluences. The same mild period lengthening was seen for all the core clock genes tested (as shown for *CCA1*, *LHY*, *PRR9*, and *PRR7*; see Supplemental Figures 3B to 3E online), indicating that *CAB2:LUC* changes are the consequence of a defective core oscillator. However, no clear change in the peak

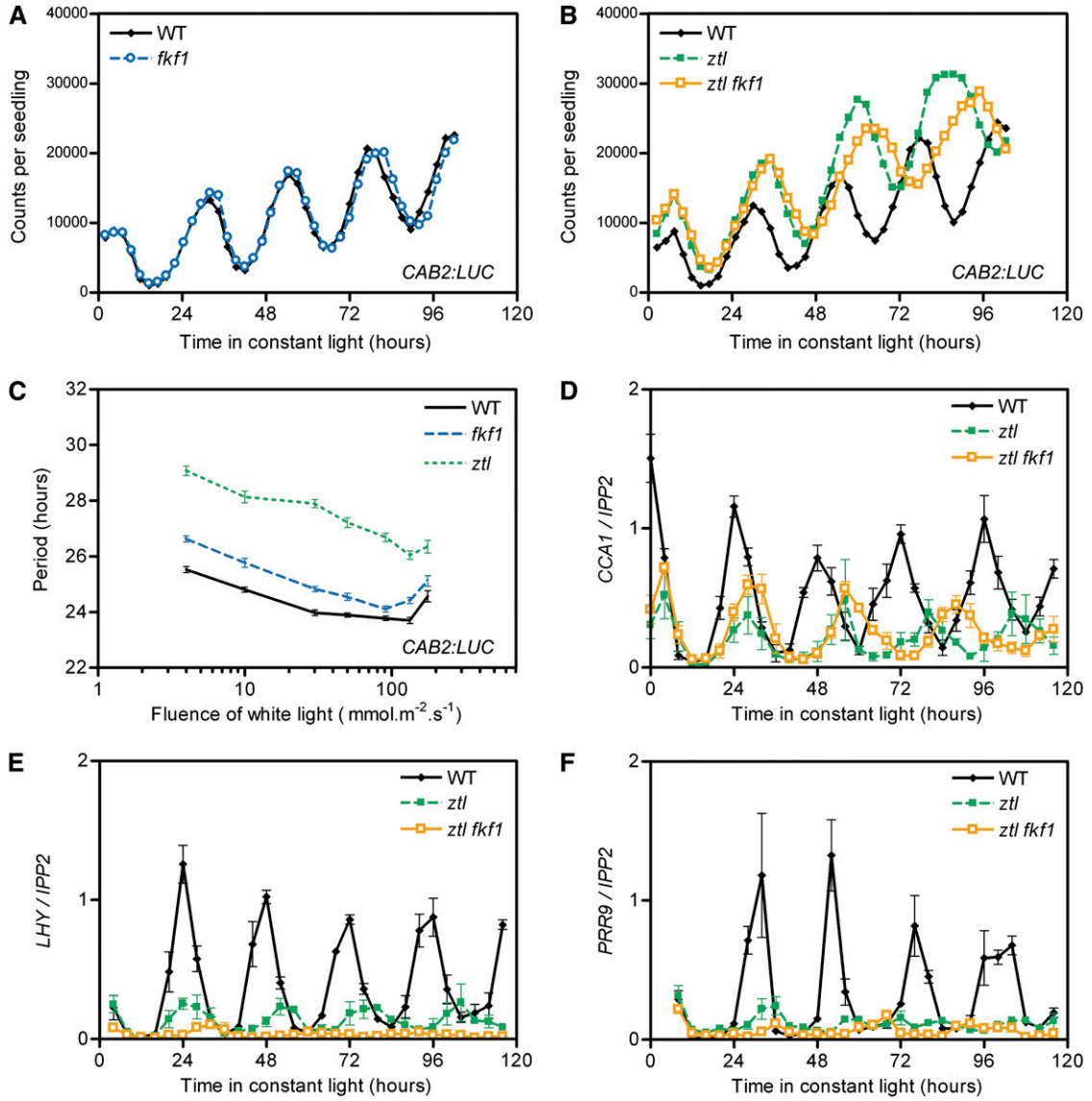

Figure 3. *fkf1* Has Mild Clock Defects but Strongly Enhances *ztl* Phenotype.

(A) to **(C)** *CAB2:LUC* activity was analyzed in wild-type, *fkf1*, *ztl*, and *ztl fkf1* genotypes in LL conditions.

(A) and **(B)** *CAB2:LUC* traces represent the average of the results obtained for 36 seedlings of each genotype and are representative of three independent experiments.

(C) The variation in *CAB2:LUC* period in wild-type, *fkf1*, and *ztl* exposed to different fluences of constant white light is presented. Each data point is the average (±SE) of the results obtained for a total of at least 50 seedlings analyzed during four independent experiments.

(D) to **(F)** *CCA1* **(D)**, *LHY* **(E)**, and *PRR9* **(F)** expressions were determined in the wild-type, *ztl*, and *ztl fkf1* genotypes. Their normalized expression levels are the average (±SE) of three independent biological replicates.

[See online article for color version of this figure.]

expression levels of the clock genes, including *LHY*, was seen in *fkf1* (see Supplemental Figure 3C online).

The *FKF1* mRNA copy number was intermediate between *ZTL* and *LKP2* levels in wild-type plants (Figure 2A). As expected (Nelson et al., 2000; Schultz et al., 2001), *FKF1* levels oscillate under circadian conditions with a peak at Zeitgeber time 8 (ZT8: 8 h after the light turns on) of 1876 copies/ng of total RNA (28% of *ZTL* mean level) and trough levels close to the *LKP2* mean level.

The *ZTL* expression level in the *fkf1* mutant was similar to that in the wild-type plants (see Supplemental Figure 1A online). The *FKF1* peak expression in the *ztl* mutant was reduced to ~40% of the wild-type level (see Supplemental Figure 1C online). However, this could be partially caused by missing the peak *FKF1* time point due to the peak shift caused by the longer period phenotype of the *ztl* mutant. Nevertheless, these results indicate that there is no obvious feedback regulation within the *ZTL* gene

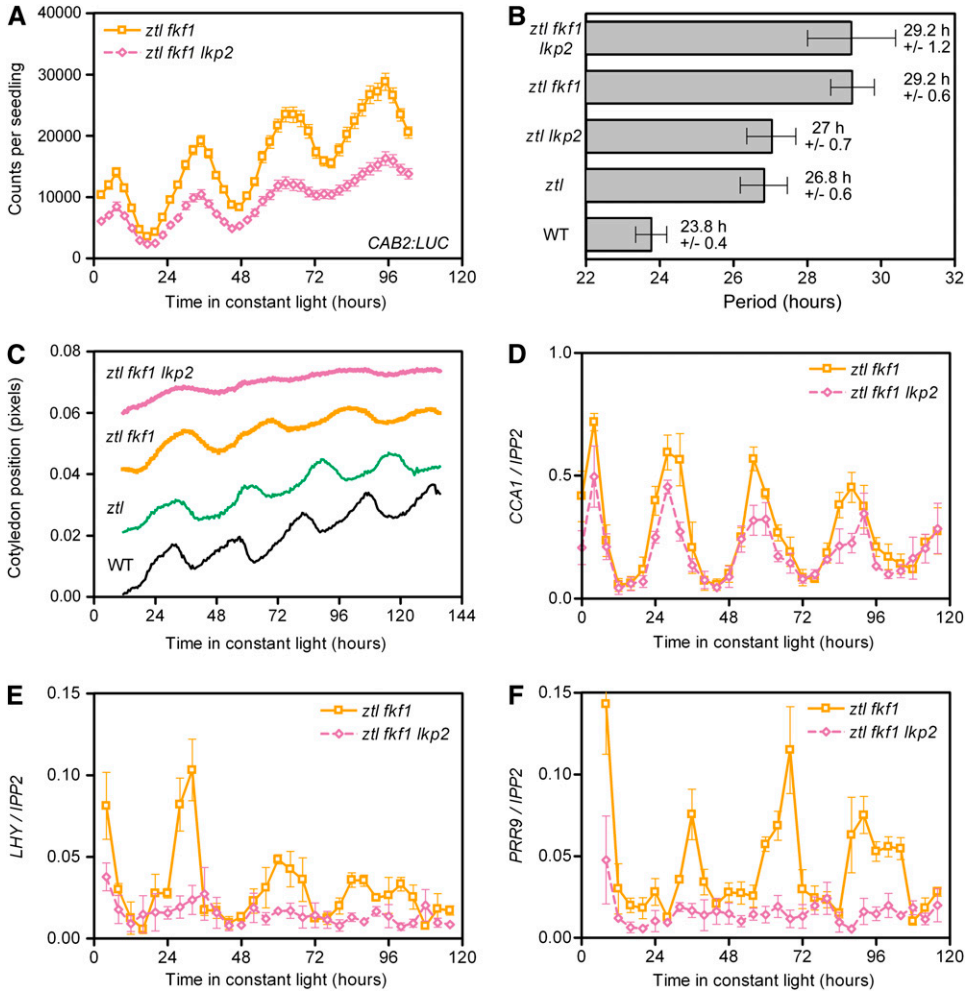

Figure 4. Comparison of *ztl fkf1* and *ztl fkf1 lkp2* Clock Phenotypes.

CAB2:LUC activity **(A)** and *CCA1* **(D)**, *LHY* **(E)**, and *PRR9* **(F)** expression were analyzed in *ztl fkf1* and *ztl fkf1 lkp2* genotypes in LL conditions.
(A) *CAB2:LUC* traces represent the average (±SE) of the results obtained for 36 seedlings of each genotype and are representative of three independent experiments.
(B) A comparison of the average period (±SDEV) of *CAB2:LUC* in the wild-type, *ztl*, *ztl lkp2*, *ztl fkf1*, and *ztl fkf1 lkp2* genotypes ($n = 36$).
(C) Results of a representative leaf movement rhythms assay experiment for wild-type ($n = 16$), *ztl* ($n = 12$), *ztl fkf1* ($n = 18$), and *ztl fkf1 lkp2* ($n = 13$) are shown.
(D) to **(F)** Normalized *CCA1* **(D)**, *LHY* **(E)**, and *PRR9* **(F)** expression levels are the average (±SE) of three independent biological replicates.
[See online article for color version of this figure.]

family to compensate for the loss of function of one or two members by increasing the gene expression of the rest. Interestingly, an increase in *FKF1* expression, when FKF1 cDNA was driven by the *ZTL* promoter, was unsuccessful in reverting the *ztl* long period (Figure 2B). This result indicates that FKF1 cannot replace the period-determining functions of ZTL. The circadian clock phenotype in the *fkf1 lkp2* mutant resembled that observed in the *fkf1* mutant (see Supplemental Figure 3 online).

ztl fkf1 lkp2 Triple Mutant Displays Weaker Rhythms Than *ztl fkf1*

To examine further the possible contribution of LKP2 to the clock progression, we analyzed the circadian clock status in the *ztl fkf1 lkp2* triple mutant by precisely comparing the rhythm alteration in this mutant to that in the *ztl fkf1* mutant. No increase was detected in the average period length of *CAB2:LUC* rhythm (Figures 4A and 4B). However, a larger standard deviation with a reduced and damping amplitude in the triple mutant suggested less robust oscillations of the clock in that mutant. The leaf movements displayed a similar tendency with much weaker oscillations in the triple mutant than in *ztl fkf1* (Figure 4C), but a rhythm was still detectable, thus confirming that the circadian clock outputs in the triple mutant are not arrhythmic. The expression of *PRR9* and *LHY* was severely repressed in the triple mutant (~2% of wild-type peak levels) and became arrhythmic in LL (Figures 4E and 4F). To a lesser extent, *PRR7* level was also slightly diminished compared with *ztl fkf1* (see Supplemental

Figure 2B online). By contrast, after 5 d in LL, *CCA1* and the evening expressed genes *TOC1* and *PRR5* displayed no significant changes other than period alterations in *ztl fkf1* and *ztl fkf1 lkp2* compared with *ztl* (Figures 3D and 4D; see Supplemental Figures 2C to 2F online).

Taken together, our results demonstrate an enhancement of the *ztl* phenotype by *fkf1* and *fkf1 lkp2*, suggesting that ZTL, FKF1, and LKP2 are all involved in the regulation of the circadian clock but that their contribution to the clock function is different with ZTL playing a more pronounced role.

FKF1, Like ZTL, Targets TOC1 and PRR5 Proteins for Degradation

To explain the action of FKF1 in the clock, we investigated its potential effect on TOC1 and PRR5 protein stabilities. Although ZTL interactions with TOC1 and PRR5 are well documented (Más et al., 2003b; Kiba et al., 2007; Kim et al., 2007), it was still unclear if FKF1 could also interact with the same targets. The TOC1–FKF1 interaction has been shown in yeast (Más et al., 2003b). Until now, no interaction has been reported between PRR5 and FKF1 (Yasuhara et al., 2004). However, under our conditions, yeast clones coexpressing FKF1 (as bait) and PRR5 (as prey) were able to grow on media selecting for the activation of the *HIS3* reporter gene, whereas the appropriate control strains did not (Figure 5A). These results suggested that a direct interaction between PRR5 and FKF1 indeed occurs, at least in yeast.

Since truncated ZTL and LKP2 proteins, including the LOV domains, are sufficient to interact with TOC1 and PRR5 in yeast (Más et al., 2003b; Yasuhara et al., 2004; Kiba et al., 2007) and the pseudoreceiver (PR) domains of both TOC1 and PRR5 are involved in the interaction with ZTL in vitro (Kiba et al., 2007; Fujiwara et al., 2008), we examined whether the same functional domains are involved in the interaction between FKF1 and TOC1/PRR5. Glutathione *S*-transferase (GST)-tagged truncated FKF1, ZTL, and LKP2 containing the N-terminal LOV domain and the F-box (LOV+F) and 6xHis-tagged PRR5 and TOC1 PR domains were produced in *Escherichia coli*. Comparable amounts of the GST-tagged proteins and His-tagged PRR5 or TOC1 were used to test whether the GST-tagged proteins copurify His-tagged PRR5 and/or TOC1 PR domains. In these experiments, all three LOV+F domain peptides, including GST-FKF1-(LOV+F),

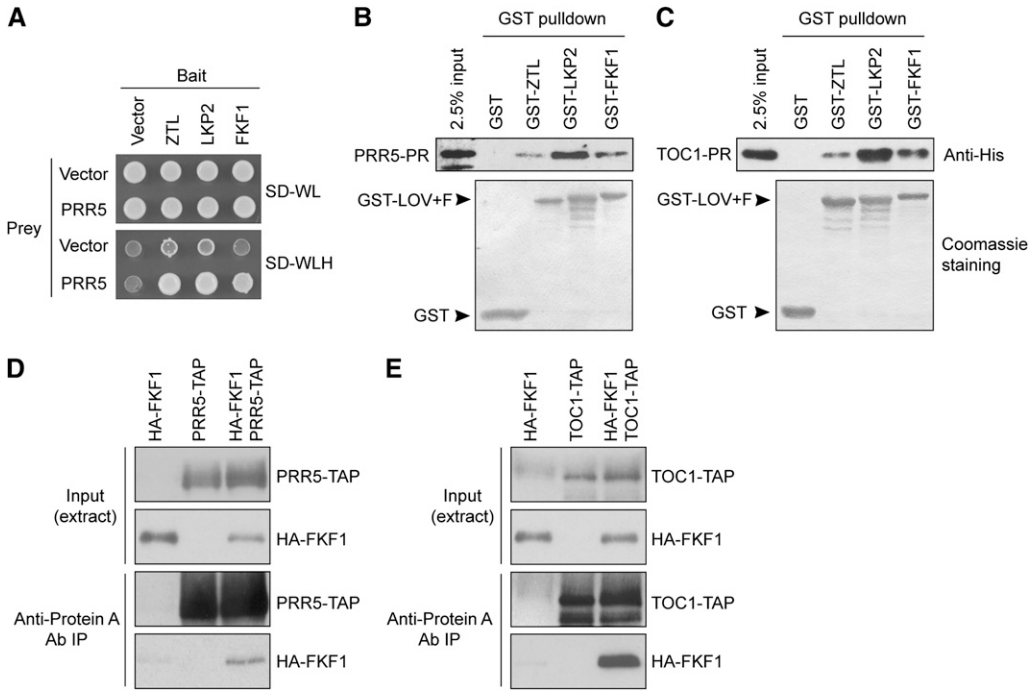

Figure 5. FKF1 Interacts with PRR5 and TOC1 Proteins.

(A) Yeast clones expressing the indicated combinations between the full-length PRR5 protein (as a prey) and the full-length ZTL, LKP2, and FKF1 proteins (as baits) were grown on appropriate media to maintain the vectors (SD-WL) and to test for the expression of the *HIS3* reporter gene for the protein–protein interaction (SD-WLH).

(B) and **(C)** Representative results of the in vitro pull-down experiments between GST alone, GST-tagged truncated versions of ZTL, FKF1, and LKP2, and the His-tagged PR domains of PRR5 **(B)** and TOC1 **(C)** are presented. Copurified PRR5-PR and TOC1-PR were detected using an anti-His antibody (top panels); 2.5% of input (top panel) and Coomassie blue staining of nitrocellulose membranes (bottom panel) display the protein amounts of His fusions, GST, and GST fusions used in these experiments.

(D) and **(E)** HA-FKF1 was coimmunoprecipitated with either PRR5-TAP **(D)** or TOC1-TAP **(E)** using an anti-Protein A antibody. The proteins were transiently expressed either alone or in combination in the presence of proteasome inhibitor MG-132 in *N. benthamiana*. The GST pull-down experiment and coimmunoprecipitation experiment were performed three times with similar results.

specifically pulled down His-PRR5-PR, thus confirming the FKF1-PRR5 interaction (Figure 5B). In a similar experiment, His-TOC1-PR also specifically associated with all GST-(LOV+F) domains (Figure 5C), indicating that these interactions are largely conserved between ZTL family proteins and PRR5/TOC1 and likely occur through the same functional domains of the proteins. We further confirmed the direct interaction of full-length FKF1 protein with both PRR5 and TOC1 proteins in planta. TAP-tagged PRR5 (PRR5-TAP), TOC1-TAP, and HA-tagged FKF1 proteins were synthesized in *Nicotiana benthamiana*. PRR5-TAP or TOC1-TAP proteins were immunoprecipitated using anti-Protein A antibody, and we analyzed whether HA-FKF1 was coimmunoprecipitated. As shown in Figures 5D and 5E, HA-FKF1 was coimmunoprecipitated with both PRR5-TAP and TOC1-TAP. We also detected the interaction of PRR5-TAP and HA-LKP2 using the same method (see Supplemental Figure 4 online). These results further suggest that FKF1 interacts with both PRR5 and TOC1 in vivo.

TOC1 and PRR5 protein oscillations are disrupted in the *ztl* mutant (Más et al., 2003b; Kiba et al., 2007; Fujiwara et al., 2008), so we used antibodies directed against the endogenous proteins (Kiba et al., 2007; Knowles et al., 2008) to compare patterns of protein accumulation in the *ztl* family mutants. To analyze possible changes in PRR5 and TOC1 protein stability in LL, independently of the potential period length differences displayed by each mutant (i.e., consecutive differences in the time of the peak), PRR5 and TOC1 protein levels were investigated during the first 28 h in LL (Figures 6C to 6F; see Supplemental Figure 5 online). As expected, a sharp peak was revealed in the wild type for PRR5 protein from ZT8 to ZT16, whereas TOC1 had a broader and later peak (detection from ZT12 to ZT24). In *ztl*, the time of the peak was mainly unchanged, but both proteins became detectable during the entire time course (although only a faint signal was seen at ZT28), consistent with ZTL being the main influence at the troughs of PRR5 and TOC1. The expression patterns of PRR5 and TOC1 proteins in *ztl lkp2* were overall similar to those in *ztl*, although the expression levels of both proteins in the double mutant seemed to be slightly higher than those in *ztl*. When *fkf1* was combined with *ztl*, an obvious increase in amounts was detected from ZT16 to ZT28 for PRR5 and at ZT24 and ZT28 for TOC1 (Figures 6E and 6F). Interestingly, this overaccumulation of PRR5 and TOC1 proteins followed the peak of transcription for both transcripts (Figures 6A and 6B) and the expected peak of cycling FKF1 protein in the wild type (Imaizumi et al., 2003). Having the *lkp2* mutation in addition to both *ztl* and *fkf1* mutations seemed to have a minor effect on PRR5 and TOC stability regulation, since we observed slightly higher levels of PRR5 and TOC1 protein accumulation in the *ztl fkf1 lkp2* mutant compared with those in the *ztl fkf1* mutant.

In contrast with the morning genes, the *TOC1* and *PRR5* transcript profiles looked similar in phase and amplitude between ZT0 and ZT28 in all mutant combinations (Figures 6A and 6B), suggesting that transcriptional difference between the lines is not a major cause for the observed differences in the protein levels. We then addressed potential changes in protein degradation by stopping translation with cycloheximide (CHX) and monitoring variations in PRR5 levels. We first tested whether a CHX treatment could stop PRR5 protein production in our conditions. As shown in Figure 7A, applying CHX at ZT0 successfully blocked the PRR5 protein accumulation at ZT8 and ZT12, demonstrating the effectiveness of the interruption of *PRR5* translation initiated by the CHX application. We then measured and compared its degradation rate among the wild-type plants, *ztl*, and *ztl fkf1 lkp2* mutants under light after treating with CHX at the peak of PRR5 accumulation (ZT12) (Figures 7B and 7C). The starting amount of PRR5 protein was very similar in these genotypes (see Supplemental Figure 6A online), but after 10 h, PRR5 almost disappeared in the wild type (reduction to 7%), whereas 30% was still detectable in *ztl* and 43% was detectable in *ztl fkf1 lkp2*. The difference in PRR5 degradation rates in these lines clearly indicates that ZTL, FKF1, and most likely LKP2 regulate the protein stability of PRR5.

TOC1 and PRR5 Are Responsible for Distinct Features of the *ztl fkf1 lkp2* Phenotype

We then analyzed whether the increased defects in TOC1 and PRR5 degradation could be responsible for the complex phenotype seen in the triple mutant. To this end, the clock phenotypes of *TOC1*- and *PRR5*-overexpressing plants as well as of the *lhy* mutant were characterized. First, a moderate *TOC1* overexpressor called *TMG* was used (Más et al., 2003a). In these plants, *TOC1* transcript level is increased to peak levels corresponding to four times wild-type levels (Figure 8A). As a consequence, the circadian oscillation in the *TMG* line is not arrhythmic like that in the strong *TOC1* overexpressing lines, but displays a long period for the core clock gene expression and all clock outputs investigated so far (Figures 8B, 8C, and 8E). Importantly, the period length in *TMG* was even slightly longer than that in *ztl* (Figures 8B, 8C, and 8E). However, the amplitude of the expressions of *LHY* and *CCA1* genes was totally unaffected, suggesting that TOC1 might be mainly responsible for the period defects seen in the triple mutant.

By contrast, *PRR5* overexpression has been shown to reduce the levels of *CCA1* and *PRR7* and has a more pronounced repression effect on *LHY* and *PRR9* (Sato et al., 2002), which is similar to the tendency observed in the triple mutant. We were wondering whether PRR5 represses the promoter activity of the morning genes or regulates the stability of their mRNAs. To answer this question, we introduced a *35S:PRR5* construct in the *LHY:LUC* and *CCA1:LUC* reporter lines. As a consequence, the activity of *LHY:LUC* was strongly attenuated, with on average a 6 times lower amplitude than in wild-type plants after 4 d in LL (Figure 9A). The *LHY:LUC* rhythms in 17 individuals out of 31 *PRR5*-overexpressing T1 plants were scored with relative amplitude error >0.5, which is indicative of weak oscillation, while the relative amplitude errors of all control plants were around 0.25, indicating robust oscillation (Figure 9C). This result suggests that overexpression of PRR5 represses *LHY* promoter activity. On the contrary, the amplitude of *CCA1:LUC* oscillation was mostly unchanged by overexpression of *PRR5* (Figure 9B), indicating that PRR5 affects the transcriptional activity of *LHY* specifically. In addition, overexpression of *PRR5* caused a weak short period phenotype. The average (±SE) of the estimated *CCA1:LUC* period length in the *PRR5* overexpressors was 22.66 ± 0.23 h, while the average period length in the control

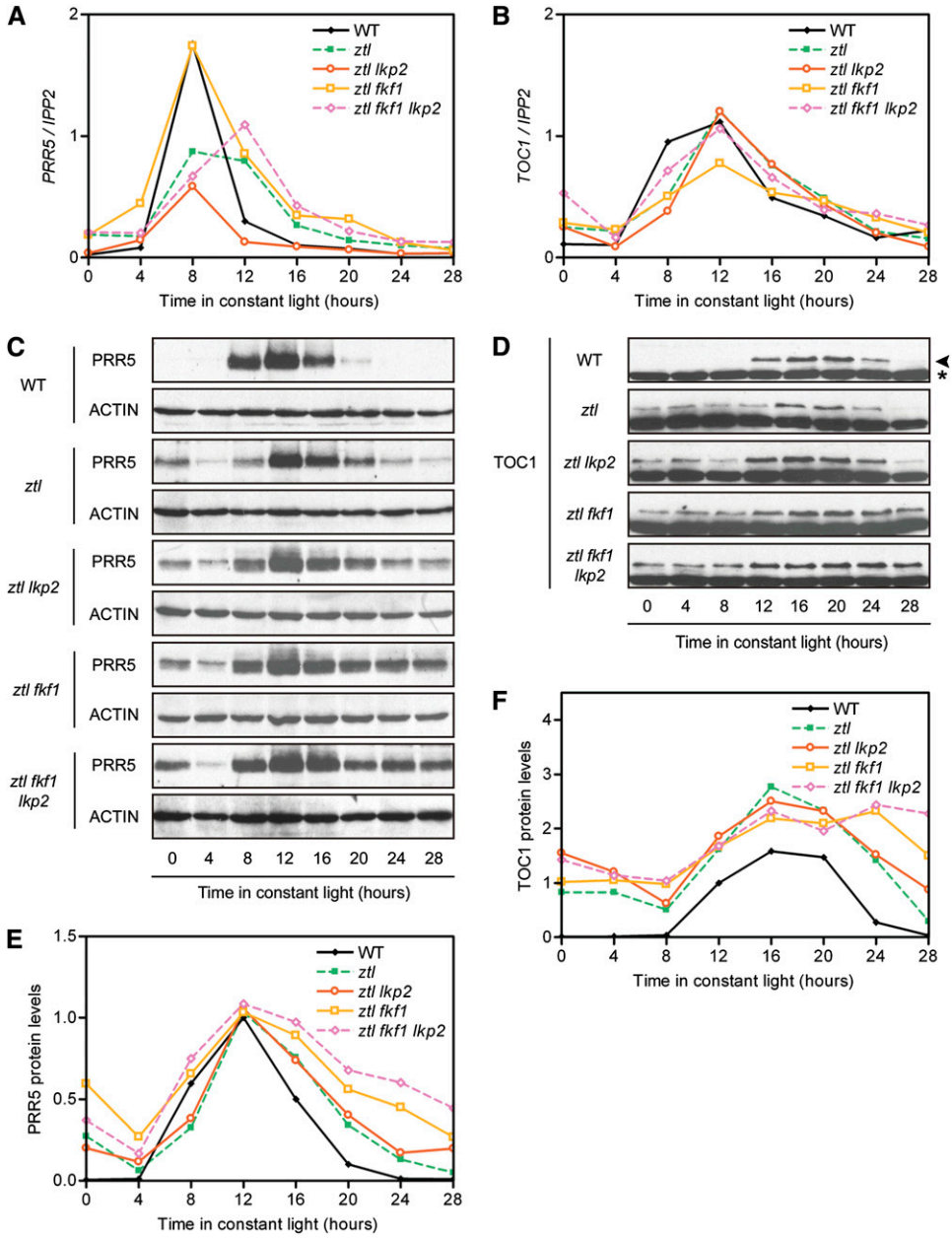

Figure 6. Patterns of PRR5 and TOC1 Oscillations in *ztl* Family Mutants.

PRR5 and *TOC1* transcript (**[A]** and **[B]**) and protein (**[C]** to **[F]**) levels were analyzed in the wild-type, *ztl*, *ztl lkp2*, *ztl fkf1*, and *ztl fkf1 lkp2* genotypes during the first 28 h in LL conditions.

(A) and **(B)** Normalized *PRR5* **(A)** and *TOC1* **(B)** expression levels are the average between three independent biological replicates (the expression patterns of both *PRR5* and *TOC1* for a full 5 d in LL conditions in the wild-type, *ztl*, *ztl fkf1*, and *ztl fkf1 lkp2* genotypes are shown in Supplemental Figure 2 online).

(C) and **(D)** The results of protein immunoblotting representative of three independent experiments are shown for PRR5 **(C)** and TOC1 **(D)** proteins. The band representing TOC1 protein is indicated by an arrowhead, while an asterisk indicates a nonspecific cross-reacting band used as a loading control.

(E) and **(F)** The relative levels of PRR5 **(E)** and TOC1 **(F)** proteins in the wild-type, *ztl*, *ztl lkp2, ztl fkf1*, and *ztl fkf1 lkp2* genotypes were determined. The value of the wild-type ZT12 time point was set as 1. The data are the means obtained from three biological replicates. The means with error bars (SE) of the same results are shown in Supplemental Figure 5 online.

[See online article for color version of this figure.]

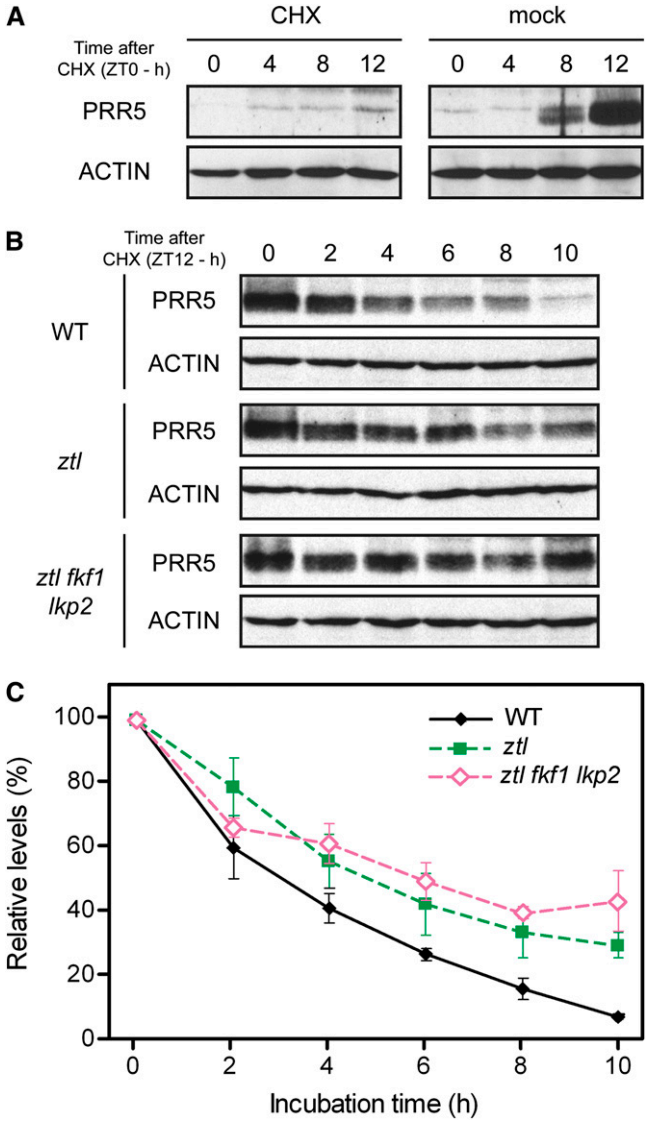

Figure 7. Comparison of PRR5 Degradation Rate in the Wild Type, *ztl*, and *ztl fkf1 lkp2*.

(A) Confirmation of the efficiency of the interruption of protein translation by CHX treatments of the wild type at the trough of PRR5 protein (ZT0). **(B)** and **(C)** PRR5 levels were measured 0, 2, 4, 6, 8, and 10 h in LL after a CHX treatment at the peak of PRR5 protein (ZT12). Representative protein immunoblotting experiments of the decreasing amounts of PRR5 in the wild type, *ztl*, and *ztl fkf1 lkp2* are shown in **(B)**. The average values (±SE) of relative change in the intensity of the bands to that of the bands at ZT12 were calculated from three independent biological replicates and are shown in **(C)**.

[See online article for color version of this figure.]

plants was 23.41 ± 0.23 h. We confirmed the reproducibility of this slight difference and also noticed that the similar weak short period phenotype of the *PRR5* overexpressor was presented previously, although it was not mentioned in the text (Sato et al., 2002). Although the period length was slightly affected in the *35S:PRR5* lines, compared with the clear period lengthening effect caused by *TOC1* overexpression (Más et al., 2003a), these results further indicate that TOC1 and PRR5 have distinct functions at the core of the oscillator.

Interestingly, the absence of *LHY* is known to affect clock progression and confers a short period phenotype. By monitoring the expression of *CCA1*, *PRR9*, and *PRR7* in *lhy* mutant plants, we found that there is also a reduction in the levels of these genes. In the *lhy* mutant, *PRR9* is reduced to 10 to 40% of the wild-type peak levels (Figure 8F), *PRR7* to 20 to 40% (see Supplemental Figure 2A online), and *CCA1* to 50% (Figure 8D). These reductions indicate that PRR5-targeted repression of *LHY* could be responsible for an indirect reduction of the other morning genes in the triple mutant. However, the *PRR9* circadian oscillation is still detectable in the *lhy* mutant, suggesting that in the triple mutant, changes other than the loss of *LHY* expression are also likely involved in the suppression of *PRR9* (cf. *PRR9* levels between Figures 4F and 8F).

Together with the results obtained from the *TMG* line and the *35S:PRR5* plants, these results indicate that PRR5 and TOC1 stabilization is a likely cause of the triple mutant circadian clock phenotype. Most importantly, here, we confirm that ZTL, FKF1, and LKP2 act on the clock by coordinately regulating the degradation of these core clock proteins.

DISCUSSION

Here, we reported that a complex redundancy mechanism resides among ZTL, FKF1, and LKP2 in the regulation of morning gene expression and in the period length determination of the oscillator. Consistent with its low expression levels, the contribution of LKP2 was observed mainly when both *ZTL* and *FKF1* were mutated. The enhanced phenotype described in the triple mutant allows us to analyze precisely the function of these proteins and their indirect effects on the clock through the degradation of TOC1 and PRR5. Interestingly, while several results suggested shared functionalities between these two PRRs, we were able to identify the main differences in their contribution to the oscillator by comparing the triple mutant phenotype to plants overexpressing either *PRR5* or *TOC1*.

Unequal Redundancy between ZTL, FKF1, and LKP2

By investigating the clock phenotype of mutant combinations among genes in the ZTL family, we uncovered a complex redundancy mechanism among ZTL, FKF1, and LKP2. ZTL was the first member identified in this conserved F-box protein subfamily to function in the clock and when mutated leads to lengthening of the period of the oscillator (Somers et al., 2000). Combined with the *fkf1* mutation, the *ztl fkf1* double mutant has an even longer period (~2 h longer when compared with the *ztl* mutant) as well as a severe reduction of *LHY* expression. Investigating the *fkf1* single mutant, we found no specific defect in the expression level of *LHY*, suggesting that ZTL function by itself is sufficient to keep the wild-type level of *LHY* expression. By contrast, a moderate light-dependent lengthening of the period observed under lower fluences suggested that a clock phenotype similar to *ztl*, but significantly weaker, exists in *fkf1*.

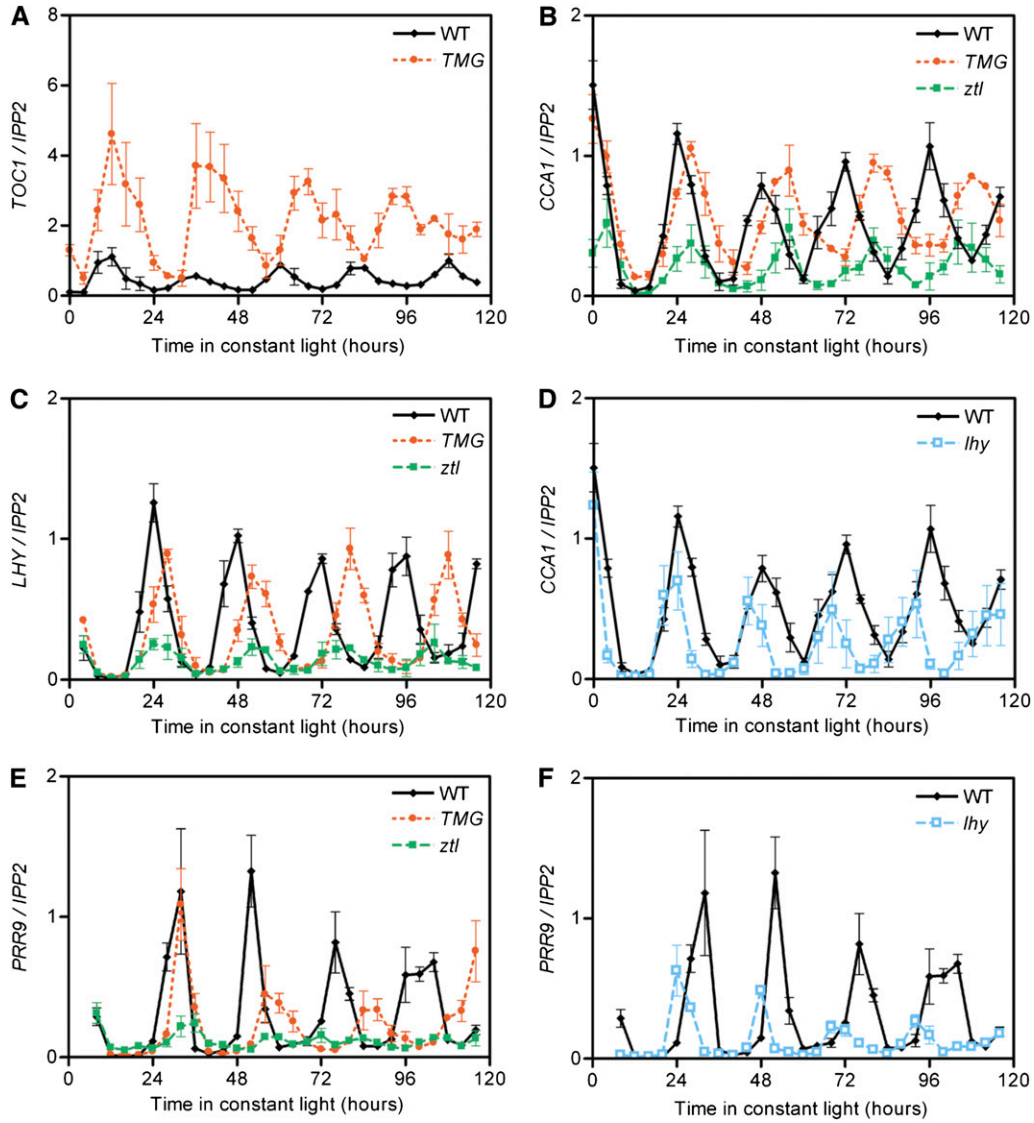

Figure 8. The *ztl fkf1 lkp2* Phenotype Can Be Distinguished from *lhy* and *TMG*.

Normalized *TOC1* **(A)**, *CCA1* (**[B]** and **[D]**), *LHY* **(C)**, and *PRR9* (**[E]** and **[F]**) expression levels are the average (±SE) between three independent biological replicates and were determined in *TMG* (**[A]** to **[C]** and **[E]**) and *lhy* (**[D]** and **[F]**) genotypes grown in LL conditions. The results obtained in the wild-type and *ztl* lines are also presented as references.
[See online article for color version of this figure.]

Consistently, the results of yeast two-hybrid, in vitro pull-down, and coimmunoprecipitation experiments indicated the ability of FKF1 to interact with TOC1 and PRR5, the main clock targets of ZTL regulation. The interaction occurred through the LOV domain of FKF1 and the PR motifs of TOC1 and PRR5, suggesting that FKF1 shares functionalities with ZTL and LKP2. In accordance with its subtle clock phenotype, no clear changes in the levels of these two target proteins were seen in *fkf1* (Kiba et al., 2007). However, an increased stabilization became obvious in *ztl fkf1* after 20 h in LL, thus demonstrating that FKF1 is an important factor in the targeted degradation of TOC1 and PRR5 when ZTL is absent. Characteristic of an unequal redundancy mechanism (Briggs et al., 2006), FKF1 clock function could be identified only in a sensitized *ztl* mutant background. This suggests that in *fkf1*, ZTL largely compensates for the absence of FKF1 in clock regulation.

However, this compensation mechanism does not account for all clock outputs. Indeed, concerning photoperiodic flowering time regulation, FKF1 has been identified as the main factor regulating the degradation of CDF1 and homologous Dof factors repressing *CO* expression (Imaizumi et al., 2005; Fornara et al., 2009). Interestingly, recent data demonstrated that the *ztl fkf1 lkp2* triple mutants flower slightly later than the *fkf1* single mutant, as a consequence of a stronger repression of *CO* expression

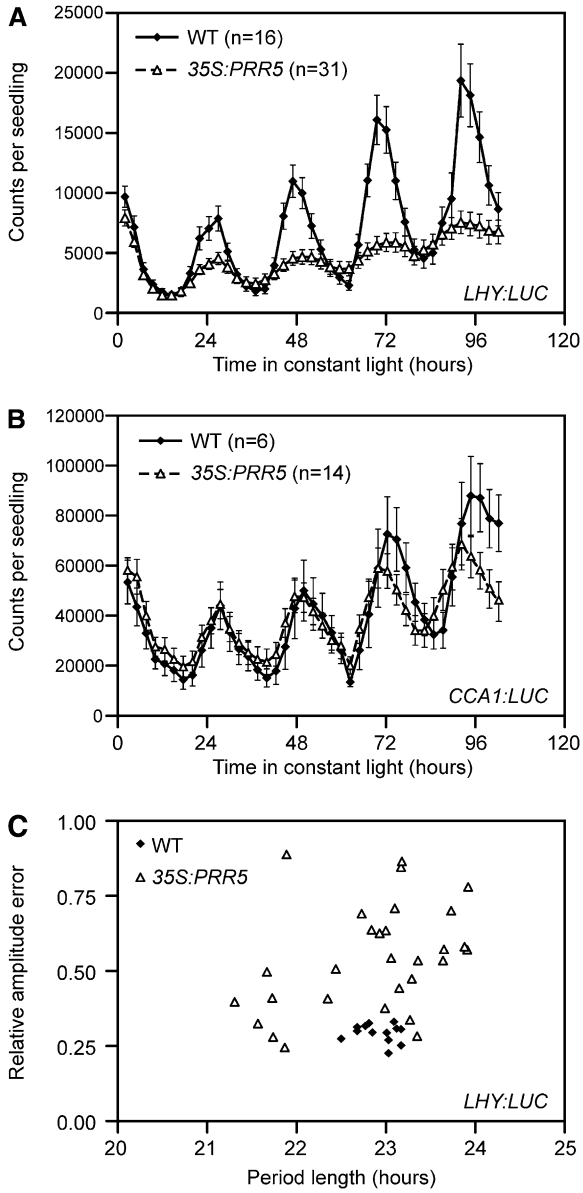

Figure 9. PRR5 Specifically Affects *LHY* Transcription.

(A) and **(B)** Plants carrying *LHY:LUC* **(A)** and *CCA1:LUC* **(B)** reporters were transformed with a *35S:PRR5* construct. Traces are the average (±SE) among the indicated numbers of transgenic lines (T1). Reporter plants transformed by an empty vector are presented as a control (WT).
(C) The scatterplot showing the Fourier transform nonlinear least square analysis (estimated period length versus relative amplitude error) of the *LHY:LUC* expression data of individual T1 seedlings used in **(A)**. Lower values in the relative amplitude error mean robust circadian oscillation.

(Fornara et al., 2009). While the transcript level of *CDF2* is reduced, a higher accumulation of CDF2 protein is detected in the triple mutant, indicating further stabilization. The molecular basis for the functional differences between FKF1 and ZTL is unclear, although affinities for their protein targets might play a role. This would partially explain the results obtained by the overexpression of FKF1 that seems unable to affect the clock, even after increased expression in a *ztl* background (Figure 2B). In the case of ZTL overexpression, an unexpected late flowering phenotype accompanied with low *CO* expression, similar to the *ztl fkf1 lkp2* triple and *gi* mutants, is observed (Somers et al., 2004). Potentially, the requirement of rate-limiting additional factors, such as GI, could account for some of these discrepancies.

In the case of LKP2, since the tissue-specific expression patterns of *ZTL*, *LKP2*, and *FKF1* seemed largely to overlap (Nelson et al., 2000; Kiyosue and Wada, 2000; Yasuhara et al., 2004), low expression might be the main explanation for the observed unequal redundancy with ZTL and FKF1 in clock regulation (Briggs et al., 2006). Functional analyses have shown a close homology with ZTL, but the proteins would not be fully equivalent, as more RNA copies of *LKP2* are required to confer a wild-type period in a *ztl* mutant background. Defects in *LKP2* would be compensated for by ZTL in *lkp2* and by FKF1 in *ztl lkp2*, as these lines were indistinguishable from the lines with *LKP2*. When compared with *ztl fkf1*, an enhancement of the clock phenotype in the triple mutant strongly suggests that LKP2 is also active in planta. *LHY* and *PRR9* levels were reduced to very low levels and became fully arrhythmic only in the triple mutant. In addition, several other outputs were more affected in this mutant, displaying weaker oscillations but only minor changes in period. In previous reports describing rhythmic plants overexpressing TOC1, the period remained below 30 h (Más et al., 2003a). This suggests that in *ztl fkf1* and the triple mutants, an upper limit to TOC1 influence on the period has been reached. Further increases in TOC1 protein levels are known to lead to arrhythmia (Makino et al., 2002; Más et al., 2003a), and the weak rhythms we characterized in this study indicate that the clock almost reached this critical stage in the triple mutant.

TOC1 and PRR5 Have Contrasting Functions in the Clock

Enhanced and novel phenotypes can be expected when combining mutations in partially redundant proteins (Briggs et al., 2006). Accordingly, our comprehensive analysis of the *ztl fkf1 lkp2* triple mutant phenotype revealed more pronounced defects in the period of the oscillator along with a strong reduction in the expression levels of the morning genes. Although a reduction in the expression of *CCA1*, *LHY*, *PRR7*, and particularly *PRR9* has been previously observed in *ztl*, the most severe defects observed in the triple mutant for *LHY* expression revealed that this morning gene is indeed one primary target of ZTL family-mediated regulation. Interestingly, the short period phenotype characteristic of *lhy* mutants is in contradiction with the lengthening of the period seen in the triple mutant and suggests that the collapse of the morning gene expression levels and the period lengthening might be two independent aspects of the triple mutant phenotype. Analysis of the *PRR5* overexpressor fully supports this hypothesis, as these plants display a strong reduction of *LHY* transcription without significant period defects (Sato et al., 2002; our study).

Both LHY and CCA1 are involved in the induction of *PRR9* and *PRR7* gene expression. Subsequently, PRR9 and PRR7 participate in repressing the expression of *LHY* and *CCA1*, resulting in

the formation of the morning feedback loop (Farré et al., 2005; Salomé and McClung, 2005). Our results suggest that PRR5 might form an additional negative feedback loop with LHY (and CCA1). Increasing PRR5 expression by introducing the *ztl* mutation reduced the expression of both *LHY* and *CCA1*, indicating that PRR5 may repress the expression of both genes. In addition, measuring *LHY* and *CCA1* levels in *ztl fkf1* and *ztl fkf1 lkp2* mutants, as well as the comparison of the activity of *LHY:LUC* and *CCA1:LUC* in *PRR5* overexpressors, indicated that further increased PRR5 protein level more strongly affects *LHY* transcription. As TOC1 protein associates with *CCA1* chromatin (Pruneda-Paz et al., 2009), it is tempting to speculate that the PRR5 effect is direct and that it may associate with the *LHY* promoter and specifically regulate its activity. Alternatively, PRR5 might also associate with *CCA1* chromatin and directly repress *CCA1* promoter activity, but an additional mechanism or factor would then counteract PRR5 mediated repression and be responsible for the maintenance of *CCA1* expression even when PRR5 protein levels are strongly elevated (as in *ztl fkf1 lkp2* triple mutant). In any case, along with the difference in the temperature effects on *CCA1* and *LHY* transcription (Gould et al., 2006) and the identification of the *CCA1*-specific regulator (Pruneda-Paz et al., 2009), our results are consistent with the existence of significant differences in the transcriptional mechanisms controlling *LHY* and *CCA1* promoter activities.

PRR5 is also involved in the regulation of the period length of the clock. The *prr5* mutant displays a slightly shorter period than do wild-type plants, and the *prr5* mutation is able to partially revert the *ztl* long-period phenotype (Kiba et al., 2007; Fujiwara et al., 2008). One explanation that could reconcile these data with our PRR5 overexpressing results would be that the observed changes are caused by an indirect effect of PRR5 on TOC1 stability. Indeed, these two proteins are degraded with a kinetic strongly depending on light and the stoichiometry of the different partners involved in this protein interaction cascade (Kiba et al., 2007; Kim et al., 2007; Fujiwara et al., 2008). One could assume that in the absence of PRR5, TOC1 degradation would be accelerated, thus indirectly conferring a short period. Consistent with this hypothesis, *prr5* effects, although similar to *toc1*, are less pronounced, as *toc1* displays a much shorter period than *prr5* that is unaffected by *ztl* mutation (Más et al., 2003b). In addition, a short period similar to the *prr5* phenotype is observed in the *prr3* single mutant, in which a mechanism specifically protecting TOC1 from degradation is impaired (Para et al., 2007; Fujiwara et al., 2008). Still, a slight reduction of *toc1* short period has been described in the *prr5 toc1* double mutant (Ito et al., 2008) that would be consistent with PRR5 sharing some functionality with TOC1. However, the *toc1* mutant used in that study (*toc1-2*) is not a null mutation, and it presents low levels of wild-type *TOC1* transcript (~5% of wild-type levels; Alabadi et al., 2001) and potentially low levels of TOC1 protein. Then, an indirect period effect of *prr5* mutation by affecting the stability of this remaining pool of TOC1 protein cannot be excluded in the *prr5 toc1* double mutant.

Conversely, a competition between TOC1 and PRR5 toward ZTL-mediated degradation might be responsible for a reduction of the levels of *CCA1*, *LHY*, and *PRR9* found in plants strongly overexpressing TOC1 (Makino et al., 2002). For that reason and to clarify the TOC1 primary function, we characterized plants with a moderate increase in TOC1 level (*TMG*; Más et al., 2003a). Although a marked lengthening of the period was seen in these plants, there was no defect in the expression levels of the morning genes, consistent with a specific effect of TOC1 on the period and a contrasted function compared with PRR5. However, the molecular mechanisms by which TOC1 affects the period remain poorly understood. Based on the reduced levels of *CCA1* and *LHY* in *toc1-2*, it was proposed to be an activator of the morning genes (Alabadi et al., 2001; Más et al., 2003a). Still, no increase in *CCA1* or *LHY* levels was seen in the *TMG* line or the triple mutant when TOC1 levels were increased. Although these data might seem inconsistent with TOC1 functioning as an activator, due to the fact that increasing the levels of CCA1 and LHY also induce a higher expression of *CCA1* and *LHY* repressors (such as PRR9 and PRR7) (Farré et al., 2005), the activation effect of TOC1 might be masked by negative feedback regulation. A strong overexpression of *CCA1* or *LHY* results in an arrhythmic oscillator (Schaffer et al., 1998; Wang and Tobin, 1998); it would be interesting to investigate the effects of a moderate increase in the levels of these genes and see if it mimics the long period of the *TMG* line. If the activation function of TOC1 is confirmed, this would indicate that ZTL-associated function has a dual outcome in releasing a strong repression mechanism (through PRR5 degradation) as well as moderating the activation of the morning genes (through TOC1 degradation). The triple mutant phenotype would then be the result of opposing forces influencing the levels of the morning genes. A better characterization of the transcription factor complexes assembling on the *CCA1* and *LHY* promoters is likely to be invaluable in deciphering the mode of action of TOC1 as well as that of PRR5, PRR7, and PRR9.

METHODS

Plant Material and Growth Conditions

The wild-type plant (Columbia [Col] background) that possesses the *CAB2:LUC* reporter was described previously (Somers et al., 1998). All single mutants *ztl-4* (Michael et al., 2003), *lkp2-1* (Imaizumi et al., 2005), *fkf1-2* (Imaizumi et al., 2003), and *lhy-20* (Michael et al., 2003) used in this study are in the Col background and have been characterized previously. The *CAB2:LUC* reporter construct was integrated into *ztl-4*, *lkp2-1*, and *fkf1-2* by genetic cross. The resulting mutant line homozygotes for the *CAB2:LUC* reporter were crossed to obtain the respective double and triple mutant combinations. The *TOC1* minigene (*TMG*) line that displays higher expression levels of *TOC1* was generated by introducing an additional copy of *TOC1* genomic sequence into wild-type (Col-0) plants (Más et al., 2003a). To generate the *LHY:LUC* reporter line, a fragment of 1689 bp upstream the *LHY* coding sequence was amplified with primers containing *Bam*HI sites (see Supplemental Table 1 online) and cloned in the *Bam*HI site of pPZPXomegaLUC+ (Schultz et al., 2001). The corresponding construct, pPZP-LHY:LUC+, was transformed into *Arabidopsis thaliana*, and bioluminescence levels were determined in several T1 transgenic lines. A *LHY:LUC* line exhibiting a luciferase expression pattern similar to the average of the T1 population analyzed was selected. The *CCA1:LUC* reporter line was previously described (Pruneda-Paz et al., 2009). For PRR5 overexpression, the full-length coding sequence of *PRR5*, including the stop codon, was amplified by specific primers (see Supplemental Table 1 online) and cloned into the pENTR/D-TOPO vector

(Invitrogen) and then recombined into the pB7WG2 binary plasmid (Karimi et al., 2002). The resulting construct was used to transform the *LHY:LUC* and *CCA1:LUC* reporter lines. Seedlings were grown on Murashige and Skoog (MS) media (MS basal salt mixture; Sigma-Aldrich) supplemented with 3% sucrose in plant incubators (Percival Scientific) under 90 $\mu mol \cdot m^{-2} \cdot s^{-1}$ of white light, unless otherwise stated.

Bioluminescence Imaging in Planta

Seedlings were grown on MS media under 12-h-light/12-h-dark photocycles (LD) for 7 d before being transferred to LL (90 $\mu mol \cdot m^{-2} \cdot s^{-1}$) conditions. For the fluence response experiment, the plants were incubated under various fluence rates of white light (4, 10, 30, 50, 90, 133, and 176 $\mu mol \cdot m^{-2} \cdot s^{-1}$) after the first 7 d of LD (90 $\mu mol \cdot m^{-2} \cdot s^{-1}$) conditions. The bioluminescence generated from the *CAB2:LUC* reporter was recorded by a CCD camera (Hamamatsu) for 25 min, every 2.5 h in a 100 h time course. Before each imaging, plants were sprayed with 1 mM luciferin (Biosynth), 0.01% Triton X-100 solution. For each seedling, the intensity of the emitted luminescence was measured using Metamorph software (Molecular Devices), and the oscillation properties (period and amplitude) were analyzed with the Biological Rhythms Analysis Software System (www.amillar.org) using fast Fourier transform nonlinear least square analysis.

mRNA Time Courses

Seedlings were grown on MS media covered with one sheet of Whatman filter paper. Two sets of seedlings were prepared for each genotype for entrainment in opposite light-dark regimes: the first set was entrained in LD (12/12) and the second set in DL (12/12). Both sets were simultaneously released in LL in the same incubator after 7 d and at a time corresponding to ZT0 for the LD-entrained seedlings or ZT12 for the DL-entrained seedlings. A 5-d time course with a 4-h resolution was then constituted by collecting seedlings from the LD-entrained set for subjective day samples (ZT0, 4, 8, 24, 28, 32, 48, 52, 56, 72, 76, 80, 96, 100, and 104) and from the DL-entrained set for subjective night samples (ZT12, 16, 20, 36, 40, 44, 60, 64, 68, 84, 88, 92, 108, 112, and 116). For each time point, 30 to 40 seedlings were harvested, immediately frozen in liquid nitrogen, and then ground frozen in a ball mill (MM301-Retsch). Total mRNA was extracted with the RNeasy plant mini kit (Qiagen), and 1 μg was used to perform the RT in 96-well plates with the iscript cDNA synthesis kit (Bio-Rad).

Specific Taqman probes (Biosearch Technologies) and primer sets were used for the quantification of *CCA1*, *LHY*, *PRR9*, *PRR7*, *PRR5*, and *TOC1* (see Supplemental Table 2 online for sequences). *IPP2*, whose expression level is not affected by either diurnal or circadian growth conditions, was used as a control representing constitutive expression. PCR reactions were performed in a MyiQ Thermal Cycler (Bio-Rad) on 2 μL of a one-tenth dilution of the product of the RT, using 1 unit of taq (Biopioneer) in the recommended buffer conditions, 0.2 mM deoxynucleotide triphosphate, and 0.3 μM of the respective Taqman probe and primers. The PCR reaction consisted of 40 cycles of 10 s denaturation at 95°C and 20 s annealing/amplification at 60°C. The resulting threshold cycle (Ct) was used for the calculation of the levels of expression relative to *IPP2*. In addition, the results were normalized by the average of circadian peak expression obtained for the wild type. In other words, the peak time points of each circadian clock–regulated gene in the wild-type time courses were selected, and the values of these time points were averaged. Then, all data point values were computed as relative values to the average of each experiment. *ZTL*, *FKF1*, and *LKP2* transcript levels were monitored using specific primer sets (see Supplemental Table 2 online) and a Sybr-Green (Invitrogen) quantification technology. PCR reactions were performed in a MyiQ Thermal Cycler on 2 μL of a one-tenth dilution of the product of the RT, using 1 unit of taq (Biopioneer), 0.2 mM deoxynucleotide triphosphate, 0.3 μM of the respective primers, 1× Sybr Green, and 10 nM fluorescein (Bio-Rad) in the recommended buffer conditions. The PCR reaction consisted of 40 cycles of 10 s denaturation, 20 s annealing at 55°C, and 20 s amplification at 72°C. Determination of the copy number was performed by comparing the Ct to a standard curve obtained for a range of dilution of *ZTL*, *FKF1*, and *LKP2* cDNA solutions of known concentrations. We also confirmed that the lowest expression levels of *LHY* and *CCA1* reported in this manuscript were still technically above the quantitative PCR detection limit (see Supplemental Figure 7 online). The primers used for the quantification of *CCA1* and *LHY* had similar linear amplification efficiencies within the ranges that we obtained, and the *LHY* levels were still above the detection limit in the *ztl fkf1 lkp2* mutant, demonstrating that our results reflect the real mRNA copy number differences of *LHY* and *CCA1* in the mutants examined.

Leaf Movement Rhythm Assay

Seedlings were germinated on MS media and entrained during 4 d in LD under white light (40 $\mu mol \cdot m^{-2} \cdot s^{-1}$) that stimulates hypocotyl elongation. After the seedlings were individually transferred to the wells of upright 24-well tissue culture plates, they were grown under constant light conditions (90 $\mu mol \cdot m^{-2} \cdot s^{-1}$), and the positions of the cotyledons were recorded. Remote shooting with a Powershot A95 camera (Canon) was started around ZT10 and lasted for 125 h with one picture taken every 30 min. Oscillations in the position of the cotyledons were analyzed using an integrated morphometry analysis with Metamorph software (Molecular Devices).

Yeast Two-Hybrid Assay

The cDNAs encoding the full length of ZTL, FKF1, and LKP2 were amplified using specific forward primers containing the *Nco*I site (the *Bsp*HI site for *LKP2*) and the reverse primers containing the *Sal*I site (see Supplemental Table 1 online) and cloned into the *Nco*I-*Sal*I sites of pGBKT7 (Clontech) for bait constructs. The *PRR5* cDNA in pENTR/D-TOPO (described in plant material and growth conditions) was inserted into the pACTGW-attR vector (pACT2 that has a Gateway cloning cassette; Nakamura et al., 2002) by Gateway LR recombination reaction (Invitrogen). pACT2 (Clontech) was used as an empty prey vector control. Detailed procedures of the yeast two-hybrid analysis were described previously (Sawa et al., 2007).

In Vitro Pull-Down Assay

Partial *ZTL*, *LKP2*, and *FKF1* sequences (nucleotide positions 1 to 765 for *ZTL*, 1 to 768 for *LKP2*, and 1 to 807 for *FKF1*; see the primer information in Supplemental Table 1 online) encoding LOV and F-box domains (LOV+F) were cloned into the GST fusion vector pDEST15 (Invitrogen) by Gateway LR recombination reaction. pGEX-4T-1 vector (Pharmacia Biotech) was used for expressing GST. *PRR5-PR* and *TOC1-PR* sequences (1 to 540 for *PRR5* and 1 to 498 for *TOC1*; see the primer information in Supplemental Table 1 online) were inserted into the pDEST17 vector (Invitrogen) for 6xHis-tag fusions. All proteins were expressed in *Escherichia coli* BL21(DE3) pLysS pRIL strain (Stratagene). GST and GST fusion proteins were immobilized to glutathione magnetic beads (Pierce).

For the PRR5 pull-down assay, glutathione beads that captured a similar amount of purified GST and GST fusion proteins were incubated with *E. coli* extracts containing 6xHis-PRR5-PR protein in binding buffer (100 mM NaCl, 50 mM Tris-HCl, pH 7.5, 5 mM EDTA, 1 mM DTT, 0.6% Triton X-100, 2.5% glycerol, and 1 mM phenylmethylsulfonyl fluoride) at 4°C for 1 h on a rotator. Four washes were performed with washing buffer (125 mM NaCl, 50 mM Tris-HCl, pH 7.5, and 0.6% Triton X-100). Pulled-down proteins were then resuspended in the SDS sample buffer and

resolved on a 10% SDS-PAGE. The presence of copurified PRR5-PR was detected by protein immunoblotting using an anti-His antibody (Genescript). For the TOC1 pull-down assay, glutathione beads with a similar amount of purified GST and GST fusion proteins were preincubated with 5 μg/μL of BSA at 4°C for 1 h. After the addition of 6xHis-TOC1-PR protein to the preincubation mixture, the incubation continued in the binding buffer (100 mM KCl, 100 mM Na_2HPO_4, 2 mM KH_2PO_4, 5 mM EDTA, 1 mM DTT, 0.6% Triton X-100, 2.5% glycerol, 1 mM PMSF, and adjusted pH to pH 7.5 by HCl) at 4°C for 1 h on a rotator. Magnetic bead-bound proteins were then pulled down, washed four times with the same buffer, and resolved on a 10% SDS-PAGE.

Coimmunoprecipitation Assay

The binary vector harboring the *35S:HA-FKF1* cassette was described previously (Sawa et al., 2007). The cDNA encoding a full length of LKP2 cloned into the pACT2 yeast two-hybrid vector (Clontech), which generates HA-tagged LKP2-GAL4 activation domain fusion protein for yeast two-hybrid analysis, was used as a PCR template. *HA-LKP2* cDNA was amplified by HA-tag and *LKP2* sequence-specific primers (see Supplemental Table 1 online) from pACT2-LKP2 and cloned into the pCR-BluntII-TOPO vector (Invitrogen). After the sequence of *HA-LKP2* was verified, the *Bsp*HI-*Bam*HI–digested fragment containing *HA-LKP2* cDNA was introduced into the *Nco*I-*Bam*HI sites of the pRTL2 vector, and the cauliflower mosaic virus 35S expression cassette excised by *Pst*I digest from the pRTL2-HA-LKP2 plasmid was cloned into the *Pst*I site of the pPZP221 binary vector. For *35S:TOC1-TAP* and *35S:PRR5-TAP* constructs, cDNA encoding full-length TOC1 and PRR5 without the stop codons, which were cloned in the pENTR/D-TOPO vector (Invitrogen), were transferred to the C-terminal TAP fusion binary vector pC-TAPi (Rohila et al., 2004) using the LR recombination reaction (Invitrogen). For transient expression, 3- to 5-week-old tobacco (*Nicotiana benthamiana*) plants grown in long-day conditions were infiltrated with *Agrobacterium tumefaciens* strain GV3101 (pMP90) harboring either HA or TAP fusion constructs or both HA and TAP fusion constructs and transferred to LD conditions. After 3 d, 10 μM of MG-132 was infiltrated into the tobacco leaves at ZT11, and tissues were harvested at ZT18. For the coimmunoprecipitation experiments, total proteins were extracted from 1 mL of ground tissues with Co-IP buffer (150 mM NaCl, 50 mM Tris-HCl, pH 7.4, 0.5% SDS, 1 mM EDTA, 3 mM DTT, Complete protease inhibitor cocktail tablet [Roche], 2 mM sodium fluoride, 2 mM sodium orthovanadate, 5% polyvinylpolypyrrolidone, and 50 μM MG-132) and incubated with 15 μL of Protein G–coupled magnetic beads (Dynabeads protein G; Invitrogen) that captured anti-Protein A antibody (Sigma-Aldrich) at 4°C for 30 min. Then the beads were washed three times with 500 μL of Co-IP buffer without MG-132, protease inhibitors, polyvinylpolypyrrolidone, and phosphatase inhibitors. Immunoprecipitated proteins were extracted with 2× SDS buffer at 80°C for 2 min, and input extracts and immunoprecipitated proteins were separated by SDS-PAGE. HA and TAP fusion proteins were detected using anti-HA antibody (3F10; Roche) and anti-Protein A antibody (Sigma-Aldrich), respectively.

ztl Complementation Constructs and Plant Transformation

The *ZTL* promoter (1667 bp in length) including the 5′ untranslated region was amplified using the ZTLp-SacI-5′ and ZTLp-XbaI-3′ primers (see Supplemental Table 1 online) to introduce restriction sites on both extremities. This fragment was cloned into the pENTR/D-TOPO vector and then excised by *Sac*I and *Xba*I digestions. It was used to replace the 35S enhancer in the pB7WG2 binary plasmid (Karimi et al., 2002) by an insertion between the compatible *Sac*I and *Spe*I sites, creating the pB7WG2-ZTLp plasmid. *ZTL* and *FKF1* cDNAs were amplified with the stop codon using the ZTL-ATG/ZTL-stop and FKF1-ATG/FKF1-stop primers and cloned into the pENTR/D-TOPO vector. Transfer of these cDNAs into pB7WG2-ZTLp was performed by a gateway LR recombination reaction (Invitrogen). Attempts to clone *LKP2* cDNA in several types of gateway-compatible vectors were unsuccessful. It was then amplified with phosphorylated ends using the LKP2-ATG-phos and LKP2-stop-phos primers and cloned directly into pB7WG2-ZTLp in which the gateway recombination cassette had been removed by an *Eco*RV digestion and the blunt ends dephosphorylated by the antarctic phosphatase (NEB). The accuracy of all cDNA and promoter constructs was confirmed by sequencing, and the resulting binary vectors allowing the transcriptional fusions between the *ZTL* promoter and *ZTL*, *FKF1*, and *LKP2* cDNAs were electroporated in the *Agrobacterium* strain GV3101 (pMP90). After an *Agrobacterium*-mediated transformation of *ztl-4* plants by the floral dip method, basta-resistant T1 seedlings were selected on MS plates containing this herbicide.

Preparation of Plant Protein Extracts and Immunoblot Analysis

Seedlings were grown under LD for 7 d before being transferred into LL. They were harvested (every 4 h for 28 h) and frozen immediately in liquid nitrogen. For the CHX experiment, seedlings were collected at the indicated ZT and incubated in a liquid MS solution containing 100 μM CHX (Kiba et al., 2007) and then harvested (every 2 h for 10 h). Frozen plant materials were ground to a fine powder and resuspended in a 1:1 ratio (w/v) with SDS loading buffer (4% SDS, 100 mM Tris-HCl, pH 6.8, 12% 2-mercaptoethanol, 20% glycerol, and 0.008% bromophenol blue). The tissue suspension was immediately incubated at 70°C for 5 min, and after centrifugation at 6000*g* for 10 min, the protein extract was collected. Protein samples (50 μg of total protein) were separated by SDS-PAGE and transferred to nitrocellulose membranes. PRR5, TOC1, and ACTIN proteins were detected using affinity-purified anti-PRR5 antibody (Kiba et al., 2007), anti-TOC1 antibody (Knowles et al., 2008), and anti-ACTIN antibody (Millipore), respectively. Horseradish peroxidase–conjugated anti-mouse IgG and anti-rabbit IgG (Thermo Fisher Scientific) were used as secondary antibodies, and Super Signal West Pico and Femto Chemiluminescent substrate kits (Thermo Fisher Scientific) were used to detect signals derived from the antibodies. All experiments were performed at least three times with independent biological replicates.

To compare PRR5 and TOC1 band intensities among mutant lines, blot images that were obtained with similar exposure times were used to quantify the band intensities. The values of the PRR5 band and TOC1 band intensity were normalized by those of the ACTIN band and the anti-TOC1 antibody cross-reacting band denoted by the asterisk in Figure 6D, respectively. Both the PRR5 and TOC1 protein levels were computed relative to the normalized signal intensity of wild-type samples harvested at ZT12. The protein level in the wild-type ZT12 time point was set to 1. To calculate the relative amount of each protein level to the wild-type ZT12 level, the ratio of the normalized values of the ZT12 band intensity from all genotypes (see the blot image in Supplemental Figure 6 online) was used to adjust the normalized value of each time point in different genotypes.

Accession Numbers

Sequence data from this article can be found in the Arabidopsis Genome Initiative data library using the following locus identifiers: *ZTL*, At5g57360; *FKF1*, At1g68050; *LKP2*, At2g18915; *TOC1*, At5g61380; *PRR5*, At5g24470; *CCA1*, At2g46830; *LHY*, At1g01060; *PRR7*, At5g02810; *PRR9*, At2g46790; and *IPP2*, At3g02780.

Supplemental Data

The following materials are available in the online version of this article.

Supplemental Figure 1. *ZTL*, *LKP2*, and *FKF1* Transcript Levels in *ztl* Family Mutant Plants.

Supplemental Figure 2. *PRR7*, *TOC1*, and *PRR5* Transcript Levels in *ztl* Family Mutant Plants.

Supplemental Figure 3. Comparison between *fkf1* and *fkf1 lkp2* Clock Phenotypes.

Supplemental Figure 4. LKP2 and PRR5 Interaction in Planta.

Supplemental Figure 5. PRR5 and TOC1 Levels in *ztl* Family Mutant Plants.

Supplemental Figure 6. Comparison of Peak Levels of PRR5 and TOC1 in *ztl* Family Mutant Plants.

Supplemental Figure 7. Amplification Efficiencies of *CCA1* and *LHY* Primer Pairs.

Supplemental Table 1. Sequence (5′→3′) of the Primers Used for Cloning in This Study.

Supplemental Table 2. Sequence (5′→3′) of the Primers and Probes Used for the Q-PCR Experiments.

ACKNOWLEDGMENTS

We thank David Somers and Norihito Nakamichi for sharing unpublished results, Michael Fromm for kindly providing pC-TAPi vector, and Tracy Larson, Steven Asbaghi, Lars Knutstad, Lauren Hsiao, Renee Kimm, Cenobio Valdivia, and Lily Quiroz for technical assistance. S.I. is supported by the Japan Society for the Promotion of Science Research Fellowships for Young Scientists. This work was supported by National Institutes of Health Grants GM044640 to N.-H.C., GM056006 and GM067837 to S.A.K., and GM079712 to T.I.

Received November 16, 2009; revised March 2, 2010; accepted March 17, 2010; published March 30, 2010.

REFERENCES

Alabadi, D., Oyama, T., Yanovsky, M.J., Harmon, F.G., Más, P., and Kay, S.A. (2001). Reciprocal regulation between *TOC1* and *LHY/CCA1* within the *Arabidopsis* circadian clock. Science **293:** 880–883.

Baudry, A., and Kay, S.A. (2008). Clock control over plant gene expression. In Advances in Botanical Research, Vol. 48, J.C. Kader and M. Delseny, eds (San Diego, CA: Elsevier), pp. 70–105.

Bell-Pedersen, D., Cassone, V.M., Earnest, D.J., Golden, S.S., Hardin, P.E., Thomas, T.L., and Zoran, M.J. (2005). Circadian rhythms from multiple oscillators: Lessons from diverse organisms. Nat. Rev. Genet. **6:** 544–556.

Bläsing, O.E., Gibon, Y., Günther, M., Höhne, M., Morcuende, R., Osuna, D., Thimm, O., Usadel, B., Scheible, W.R., and Stitt, M. (2005). Sugars and circadian regulation make major contributions to the global regulation of diurnal gene expression in *Arabidopsis.* Plant Cell **17:** 3257–3281.

Briggs, G.C., Osmont, K.S., Shindo, C., Sibout, R., and Hardtke, C.S. (2006). Unequal genetic redundancies in Arabidopsis–A neglected phenomenon? Trends Plant Sci. **11:** 492–498.

Covington, M.F., Panda, S., Liu, X.L., Strayer, C.A., Wagner, D.R., and Kay, S.A. (2001). ELF3 modulates resetting of the circadian clock in *Arabidopsis*. Plant Cell **13:** 1305–1315.

Dharmasiri, N., Dharmasiri, S., Weijers, D., Lechner, E., Yamada, M., Hobbie, L., Ehrismann, J.S., Jürgens, G., and Estelle, M. (2005). Plant development is regulated by a family of auxin receptor F box proteins. Dev. Cell **9:** 109–119.

Dodd, A.N., Salathia, N., Hall, A., Kévei, E., Tóth, R., Nagy, F., Hibberd, J.M., Millar, A.J., and Webb, A.A. (2005). Plant circadian clocks increase photosynthesis, growth, survival, and competitive advantage. Science **309:** 630–633.

Doyle, M.R., Davis, S.J., Bastow, R.M., McWatters, H.G., Kozma-Bognár, L., Nagy, F., Millar, A.J., and Amasino, R.M. (2002). The *ELF4* gene controls circadian rhythms and flowering time in *Arabidopsis thaliana.* Nature **419:** 74–77.

Farré, E.M., Harmer, S.L., Harmon, F.G., Yanovsky, M.J., and Kay, S.A. (2005). Overlapping and distinct roles of *PRR7* and *PRR9* in the *Arabidopsis* circadian clock. Curr. Biol. **15:** 47–54.

Fornara, F., Panigrahi, K.C., Gissot, L., Sauerbrunn, N., Rühl, M., Jarillo, J.A., and Coupland, G. (2009). *Arabidopsis* DOF transcription factors act redundantly to reduce *CONSTANS* expression and are essential for a photoperiodic flowering response. Dev. Cell **17:** 75–86.

Fujiwara, S., Wang, L., Han, L., Suh, S.S., Salomé, P.A., McClung, C.R., and Somers, D.E. (2008). Post-translational regulation of the *Arabidopsis* circadian clock through selective proteolysis and phosphorylation of pseudo-response regulator proteins. J. Biol. Chem. **283:** 23073–23083.

Fukamatsu, Y., Mitsui, S., Yasuhara, M., Tokioka, Y., Ihara, N., Fujita, S., and Kiyosue, T. (2005). Identification of LOV KELCH PROTEIN2 (LKP2)-interacting factors that can recruit LKP2 to nuclear bodies. Plant Cell Physiol. **46:** 1340–1349.

Gould, P.D., Locke, J.C.W., Larue, C., Southern, M.M., Davis, S.J., Hanano, S., Moyle, R., Milich, R., Putterill, J., Millar, A.J., and Hall, A. (2006). The molecular basis of temperature compensation in the *Arabidopsis* circadian clock. Plant Cell **18:** 1177–1187.

Green, R.M., Tingay, S., Wang, Z.-Y., and Tobin, E.M. (2002). Circadian rhythms confer a higher level of fitness to Arabidopsis plants. Plant Physiol. **129:** 576–584.

Harmer, S.L. (2009). The circadian system in higher plants. Annu. Rev. Plant Biol. **60:** 357–377.

Hazen, S.P., Schultz, T.F., Pruneda-Paz, J.L., Borevitz, J.O., Ecker, J.R., and Kay, S.A. (2005). *LUX ARRHYTHMO* encodes a Myb domain protein essential for circadian rhythms. Proc. Natl. Acad. Sci. USA **102:** 10387–10392.

Imaizumi, T. (2010). *Arabidopsis* circadian clock and photoperiodism: Time to think about location. Curr. Opin. Plant Biol. **13:** 83–89.

Imaizumi, T., Schultz, T.F., Harmon, F.G., Ho, L.A., and Kay, S.A. (2005). FKF1 F-box protein mediates cyclic degradation of a repressor of *CONSTANS* in *Arabidopsis.* Science **309:** 293–297.

Imaizumi, T., Tran, H.G., Swartz, T.E., Briggs, W.R., and Kay, S.A. (2003). FKF1 is essential for photoperiodic-specific light signalling in *Arabidopsis.* Nature **426:** 302–306.

Ito, S., Niwa, Y., Nakamichi, N., Kawamura, H., Yamashino, T., and Mizuno, T. (2008). Insight into missing genetic links between two evening-expressed pseudo-response regulator genes *TOC1* and *PRR5* in the circadian clock-controlled circuitry in *Arabidopsis thaliana.* Plant Cell Physiol. **49:** 201–213.

Karimi, M., Inzé, D., and Depicker, A. (2002). GATEWAY vectors for *Agrobacterium*-mediated plant transformation. Trends Plant Sci. **7:** 193–195.

Kiba, T., Henriques, R., Sakakibara, H., and Chua, N.H. (2007). Targeted degradation of PSEUDO-RESPONSE REGULATOR5 by an SCF^{ZTL} complex regulates clock function and photomorphogenesis in *Arabidopsis thaliana.* Plant Cell **19:** 2516–2530.

Kim, W.Y., Fujiwara, S., Suh, S.S., Kim, J., Kim, Y., Han, L., David, K., Putterill, J., Nam, H.G., and Somers, D.E. (2007). ZEITLUPE is a circadian photoreceptor stabilized by GIGANTEA in blue light. Nature **449:** 356–360.

Kiyosue, T., and Wada, M. (2000). LKP1 (LOV kelch protein 1): A factor involved in the regulation of flowering time in Arabidopsis. Plant J. **23:** 807–815.

Knowles, S.M., Lu, S.X., and Tobin, E.M. (2008). Testing time: Can ethanol-induced pulses of proposed oscillator components phase shift rhythms in *Arabidopsis?* J. Biol. Rhythms **23:** 463–471.

Makino, S., Kiba, T., Imamura, A., Hanaki, N., Nakamura, A., Suzuki, T., Taniguchi, M., Ueguchi, C., Sugiyama, T., and Mizuno, T. (2000). Genes encoding pseudo-response regulators: insight into His-to-Asp phosphorelay and circadian rhythm in *Arabidopsis thaliana.* Plant Cell Physiol. **41:** 791–803.

Makino, S., Matsushika, A., Kojima, M., Yamashino, T., and Mizuno, T. (2002). The APRR1/TOC1 quintet implicated in circadian rhythms of *Arabidopsis thaliana*: I. Characterization with APRR1-overexpressing plants. Plant Cell Physiol. **43:** 58–69.

Más, P. (2008). Circadian clock function in *Arabidopsis thaliana*: Time beyond transcription. Trends Cell Biol. **18:** 273–281.

Más, P., Alabadi, D., Yanovsky, M.J., Oyama, T., and Kay, S.A. (2003a). Dual role of TOC1 in the control of circadian and photomorphogenic responses in *Arabidopsis*. Plant Cell **15:** 223–236.

Más, P., Kim, W.Y., Somers, D.E., and Kay, S.A. (2003b). Targeted degradation of TOC1 by ZTL modulates circadian function in *Arabidopsis thaliana.* Nature **426:** 567–570.

Michael, T.P., et al. (2008). Network discovery pipeline elucidates conserved time-of-day-specific *cis*-regulatory modules. PLoS Genet. **4:** e14.

Michael, T.P., Salomé, P.A., Yu, H.J., Spencer, T.R., Sharp, E.L., McPeek, M.A., Alonso, J.M., Ecker, J.R., and McClung, C.R. (2003). Enhanced fitness conferred by naturally occurring variation in the circadian clock. Science **302:** 1049–1053.

Nakamura, M., Kikuno, R., and Ohara, O. (2002). Protein-protein interactions between large proteins: Two-hybrid screening using a functionally classified library composed of long cDNAs. Genome Res. **11:** 1773–1784.

Nelson, D.C., Lasswell, J., Rogg, L.E., Cohen, M.A., and Bartel, B. (2000). *FKF1*, a clock-controlled gene that regulates the transition to flowering in *Arabidopsis.* Cell **101:** 331–340.

Ni, Z., Kim, E.D., Ha, M., Lackey, E., Liu, J., Zhang, Y., Sun, Q., and Chen, Z.J. (2009). Altered circadian rhythms regulate growth vigor in hybrids and allopolyploids. Nature **457:** 327–331.

Para, A., Farré, E.M., Imaizumi, T., Pruneda-Paz, J.L., Harmon, F.G., and Kay, S.A. (2007). PRR3 is a vascular regulator of TOC1 stability in the *Arabidopsis* circadian clock. Plant Cell **19:** 3462–3473.

Perales, M., and Más, P. (2007). A functional link between rhythmic changes in chromatin structure and the *Arabidopsis* biological clock. Plant Cell **19:** 2111–2123.

Pruneda-Paz, J.L., Breton, G., Para, A., and Kay, S.A. (2009). A functional genomics approach reveals CHE as a component of the *Arabidopsis* circadian clock. Science **323:** 1481–1485.

Qiao, H., Chang, K.N., Yazaki, J., and Ecker, J.R. (2009). Interplay between ethylene, ETP1/ETP2 F-box proteins, and degradation of EIN2 triggers ethylene responses in *Arabidopsis.* Genes Dev. **23:** 512–521.

Rohila, J.S., Chen, M., Cerny, R., and Fromm, M.E. (2004). Improved tandem affinity purification tag and methods for isolation of protein heterocomplexes from plants. Plant J. **38:** 172–181.

Salomé, P.A., and McClung, C.R. (2005). *PSEUDO-RESPONSE REGULATOR 7* and *9* are partially redundant genes essential for the temperature responsiveness of the *Arabidopsis* circadian clock. Plant Cell **17:** 791–803.

Sato, E., Nakamichi, N., Yamashino, T., and Mizuno, T. (2002). Aberrant expression of the *Arabidopsis* circadian-regulated *APRR5* gene belonging to the APRR1/TOC1 quintet results in early flowering and hypersensitiveness to light in early photomorphogenesis. Plant Cell Physiol. **43:** 1374–1385.

Sawa, M., Nusinow, D.A., Kay, S.A., and Imaizumi, T. (2007). FKF1 and GIGANTEA complex formation is required for day-length measurement in *Arabidopsis.* Science **318:** 261–265.

Schaffer, R., Ramsay, N., Samach, A., Corden, S., Putterill, J., Carré, I.A., and Coupland, G. (1998). The *late elongated hypocotyl* mutation of *Arabidopsis* disrupts circadian rhythms and the photoperiodic control of flowering. Cell **93:** 1219–1229.

Schultz, T.F., Kiyosue, T., Yanovsky, M., Wada, M., and Kay, S.A. (2001). A role for LKP2 in the circadian clock of *Arabidopsis*. Plant Cell **13:** 2659–2670.

Schwager, K.M., Calderon-Villalobos, L.I., Dohmann, E.M., Willige, B.C., Knierer, S., Nill, C., and Schwechheimer, C. (2007). Characterization of the *VIER F-BOX PROTEINE* genes from *Arabidopsis* reveals their importance for plant growth and development. Plant Cell **19:** 1163–1178.

Somers, D.E., Devlin, P.F., and Kay, S.A. (1998). Phytochromes and cryptochromes in the entrainment of the *Arabidopsis* circadian clock. Science **282:** 1488–1490.

Somers, D.E., Kim, W.Y., and Geng, R. (2004). The F-box protein ZEITLUPE confers dosage-dependent control on the circadian clock, photomorphogenesis, and flowering time. Plant Cell **16:** 769–782.

Somers, D.E., Schultz, T.F., Milnamow, M., and Kay, S.A. (2000). *ZEITLUPE* encodes a novel clock-associated PAS protein from *Arabidopsis.* Cell **101:** 319–329.

Strayer, C., Oyama, T., Schultz, T.F., Raman, R., Somers, D.E., Más, P., Panda, S., Kreps, J.A., and Kay, S.A. (2000). Cloning of the *Arabidopsis* clock gene *TOC1*, an autoregulatory response regulator homolog. Science **289:** 768–771.

Wang, Z.Y., and Tobin, E.M. (1998). Constitutive expression of the *CIRCADIAN CLOCK ASSOCIATED 1* (*CCA1*) gene disrupts circadian rhythms and suppresses its own expression. Cell **93:** 1207–1217.

Wijnen, H., and Young, M.W. (2006). Interplay of circadian clocks and metabolic rhythms. Annu. Rev. Genet. **40:** 409–448.

Xu, G., Ma, H., Nei, M., and Kong, H. (2009). Evolution of F-box genes in plants: Different modes of sequence divergence and their relationships with functional diversification. Proc. Natl. Acad. Sci. USA **106:** 835–840.

Yasuhara, M., Mitsui, S., Hirano, H., Takanabe, R., Tokioka, Y., Ihara, N., Komatsu, A., Seki, M., Shinozaki, K., and Kiyosue, T. (2004). Identification of ASK and clock-associated proteins as molecular partners of LKP2 (LOV kelch protein 2) in *Arabidopsis.* J. Exp. Bot. **55:** 2015–2027.